AD-A045 425 DAVID W TAYLOR NAVAL SHIP RESEARCH AND DEVELOPMENT CE--ETC F/G 20/4
ASSESSMENT OF LOAD ALLEVIATION DEVICES INSTALLED ON A POWER-AUG--ETC(U)
AUG 77 E F MCCABE

UNCLASSIFIED DTNSRDC/ASED-383 NL

| OF |
AD
A045425

END
DATE
FILMED
11 -77
DDC

(12)
B.S.

ASSESSMENT OF LOAD ALLEVIATION DEVICES INSTALLED ON A POWER-AUGMENTED-RAM WING OVER IRREGULAR WAVES

by

Earl F. McCabe, Jr.

AVIATION AND SURFACE EFFECTS DEPARTMENT

DTNSRDC ASED-383

August 1977

DAVID W. TAYLOR NAVAL SHIP RESEARCH AND DEVELOPMENT CENTER

BETHESDA MARYLAND 20084

UNCLASSIFIED

SECURITY CLASSIFICATION OF THIS PAGE (When Data Entered)

REPORT DOCUMENTATION PAGE

READ INSTRUCTIONS BEFORE COMPLETING FORM

(14) 1. REPORT NUMBER: DTNSRDC/ASED-383 | 2. GOVT ACCESSION NO. | (9) 3. RECIPIENT'S CATALOG NUMBER

(6) 4. TITLE (and Subtitle): ASSESSMENT OF LOAD ALLEVIATION DEVICES INSTALLED ON A POWER-AUGMENTED-RAM WING OVER IRREGULAR WAVES

5. TYPE OF REPORT & PERIOD COVERED: Final Report, Oct 1976 - Aug 1977

6. PERFORMING ORG. REPORT NUMBER

(10) 7. AUTHOR(s): Earl F. McCabe, Jr

8. CONTRACT OR GRANT NUMBER(s)

(16) 9. PERFORMING ORGANIZATION NAME AND ADDRESS: David W. Taylor Naval Ship Research and Development Center, Bethesda, Maryland 20084

10. PROGRAM ELEMENT, PROJECT, TASK AREA & WORK UNIT NUMBERS: Program Element 63534N, Task Area SSH15002, Work Unit 1612-008

(11) 11. CONTROLLING OFFICE NAME AND ADDRESS: Commander, Naval Air Development Center, Warminster, Pennsylvania 18974

12. REPORT DATE: August 1977

13. NUMBER OF PAGES: 69

(12) 74p.

14. MONITORING AGENCY NAME & ADDRESS (if different from Controlling Office)

15. SECURITY CLASS. (of this report): UNCLASSIFIED

15a. DECLASSIFICATION/DOWNGRADING SCHEDULE

16. DISTRIBUTION STATEMENT (of this Report)

Approved for Public Release: Distribution Unlimited

(17) SSH15002

DDC RECEIVED OCT 21 1977 B

17. DISTRIBUTION STATEMENT (of the abstract entered in Block 20, if different from Report)

18. SUPPLEMENTARY NOTES

Wing-in-Ground
Endplates
Load Alleviation Devices
Power-Augmented-Ram

19. KEY WORDS (Continue on reverse side if necessary and identify by block number)

20. ABSTRACT (Continue on reverse side if necessary and identify by block number)

An investigation was conducted on Carriage III at the David W. Taylor Naval Ship Research and Development Center to determine the motions and performance of a power-augmented, wing-in-ground-effect model with load alleviation devices. The effects of soft and bumpered endplates and a flexible flap were investigated for a range of velocities, thrust-to-weight ratios, and irregular wave sea states. Results show that the flexible flap can provide a smoother, softer ride for a thrust-to-weight ratio of 0.20, but at

(Continued on reverse side)

over

DD FORM 1 JAN 73 1473 EDITION OF 1 NOV 65 IS OBSOLETE S/N 0102-014-6601

UNCLASSIFIED

SECURITY CLASSIFICATION OF THIS PAGE (When Data Entered)

387695

(Block 20 continued)

the expense of decreased average heave and increased average drag. Results also indicate a transport efficiency degradation from 23.18 to 10.06 with increase in sea state from 0 to 5 for the model without load alleviation. The results are inconclusive for the soft and bumpered endplates.

TABLE OF CONTENTS

	Page
ABSTRACT	1
ADMINISTRATIVE INFORMATION	1
INTRODUCTION	1
BACKGROUND	1
OBJECTIVE	2
APPARATUS	3
MODEL	3
DATA REDUCTION	5
EFFECT OF PRESSURE VARIATION IN FLEXIBLE FLAP	7
EFFECTIVENESS OF FLEXIBLE FLAP	7
EFFECT OF SEA STATE ON MODEL WITHOUT LOAD ALLEVIATION	7
EFFECT OF PRESSURE VARIATION IN SOFT ENDPLATES	9
EFFECT OF SEA STATE ON SOFT ENDPLATES	9
EFFECT OF THRUST-TO-WEIGHT RATIO ON SOFT ENDPLATES	10
EFFECTIVENESS OF SOFT ENDPLATES	11
EFFECT OF SPRING STIFFNESS ON BUMPERS/SPRINGS ENDPLATES	11
EFFECTIVENESS OF BUMPERS/SPRINGS ENDPLATES	12
EFFECT OF SEA STATE ON BASIC RIGID ENDPLATES	13
EFFECT OF THRUST-TO-WEIGHT RATIO ON BASIC RIGID ENDPLATES	14
CONCLUSIONS	14
RECOMMENDATIONS	15

LIST OF FIGURES

	Page
1 - PAR-WIG Model on Carriage III Support System	16
2 - General Arrangement of PAR-WIG Model	17
3 - Model Flap Configurations	18
4 - Model Endplate Configurations	19
5 - Endplates Removed from Model	20
6 - Flexible Flap Pressures for T/W = 0.25 at Sea State 5	22
7 - Rigid Versus Flexible Flap for T/W = 0.20 at Sea State 5	26
8 - Metal Endplate with Rigid Flap for T/W = 0.20 at Sea States 0 and 5	30
9 - Metal Endplate with Rigid Flap for T/W = 0.25 at Sea State 5	35
10 - Soft Endplate for T/W = 0.25 at Sea States 0, 4, and 5	39
11 - Soft Endplate for T/W = 0.20 Versus T/W = 0.25 at Sea State 5	43
12 - Basic Rigid Versus Soft Endplate for T/W = 0.25 at Sea State 5	47
13 - Two-Spring Bumper with Various Stiffnesses for T/W = 0.25 at Sea State 5	51
14 - Basic Rigid Endplate for T/W = 0.25 at Sea States 0, 4, and 5	55
15 - Basic Rigid Endplate for T/W = 0.20 Versus T/W = 0.25 at Sea State 0	59

LIST OF TABLES

1 - PAR-WIG Model Information	61
2 - Single Sample Accuracy	63
3 - Effect of Sea State on Performance of Model without Load Alleviation	64

NOTATION

Accel	Center-of-gravity (C.G.) acceleration, gravitational units (G)
A/R	Aspect ratio
A_j	Ducted-fan propulsor jet area, ft^2 (m^2)
a	Width of endplate, in. (cm)
Cruise	Optimum conditions for sustained travel, conditions of thrust equals drag and lift equals model weight
c	Wing (including flap) portion chord, in. (cm)
Drag	Actual model drag corrected for thrust alignment and calibration interaction, positive aft, lb (kg)
d	Depth from wing bottom surface to endplate bottom, in. (cm)
Gage	Block gage drag which includes propulsor fan thrust, model drag, and calibration interaction, positive aft, lb (kg)
Heave	Height of wing bottom surface from mean waterline, positive above water, in. (cm)
ℓ_{ep}	Horizontal length of endplate at maximum section, in. (cm)
ℓ	Horizontal length of endplate bottom edge, in. (cm)
Mean	Time average data value
P	Total propulsive power, ft-lb/sec (W)
rms	Root-mean-square, square root of the average squared data
rpm	Revolutions per minute
$\text{Thrust}_{\text{Speed}}$	Calculated total propulsor fan thrust corrected for velocity effects, positive forward, lb (kg)
T/W	Thrust-to-weight ratio
Velocity, V	Mean model (carriage) velocity, positive forward, ft/sec (km/hr)
V_j	Ducted-fan propulsor jet velocity, ft/sec (km/hr)
η_T	Transport efficiency, W·V/P
θ_F	Fan angle indicating thrust orientation, positive upward from a mean waterline, deg
ρ	Air density, $lb\text{-}sec^2/ft^4$ (kg/m^3)

ABSTRACT

An investigation was conducted on Carriage III at the David W. Taylor Naval Ship Research and Development Center to determine the motions and performance of a power-augmented, wing-in-ground-effect model with load alleviation devices. The effects of soft and bumpered endplates and a flexible flap were investigated for a range of velocities, thrust-to-weight ratios, and irregular wave sea states. Results show that the flexible flap can provide a smoother, softer ride for a thrust-to-weight ratio of 0.20, but at the expense of decreased average heave and increased average drag. Results also indicate a transport efficiency degradation from 23.18 to 10.06 with increase in sea state from 0 to 5 for the model without load alleviation. The results are inconclusive for the soft and bumpered endplates.

ADMINISTRATIVE INFORMATION

This parametric investigation was undertaken by the Air ANVCE Projects Division (1612) of the Aviation and Surface Effects Department (16) of the David W. Taylor Naval Ship Research and Development Center (DTNSRDC). The program was sponsored by the Naval Air Development Center and was funded under Task Area SSH15002, Work Unit 1612-008.

INTRODUCTION

BACKGROUND

Studies to determine the military worth, technical feasibility, and cost of advanced wing-in-ground (WIG) effect vehicles have been progressing under the auspices of the ANVCE Project Office since September 1975. In

addition to analytical studies,[1,2] the studies included parametric investigations of WIG performance over a stationary ground board at DTNSRDC commencing in April 1976. Studies continued with WIG performance investigations over calm water at the DTNSRDC Langley Tank 1 from July through August 1976; most recent performance investigations have been conducted over waves of various sea states at the DTNSRDC Carriage III.* This report analyzes a portion of the most recent data taken for load alleviation devices over both calm water and irregular head seas.

One of the major problems besetting the power-augmented-ram (PAR) WIG success is the additional structure required to provide the size, strength, and weight necessary to withstand water impact. The maximum loads anticipated are from impacting irregular waves in a high sea state. To address this problem, load alleviation devices were conceived for investigation by a model experiment.

OBJECTIVE

The primary objective of this report is to assess the effectiveness of three load alleviation devices on a PAR-WIG model accelerating over irregular waves of various sea states. The three devices are a flexible air-bag flap, a soft air-filled fingered endplate, and a sprung forebody-planing-surface endplate. The secondary objective of this report is to determine the effect of sea state on the efficiency of the model without load alleviation.

---

[1]Gallington, R. W., "Sudden Deceleration of a Free Jet at the Entrance of a Channel," DTNSRDC Report ASED 350 (Jan 1976).

[2]Gallington, R. W. and H. R. Chaplin, "Theory of Power Augmented Ram Lift at Zero Forward Speed," DTNSRDC Report ASED 365 (Feb 1976).

*Reported informally by F. Krause ("Parametric Investigation of a Power-Augmented Ram Wing over Water," DTNSRDC ASED TM-16-76-95, Oct 1976) and E. McCabe ("Parametric Investigation of a Power Augmented Ram Wing with Load Alleviation Devices over Water Waves of Various Sea States," DTNSRDC ASED TM-16-76-97, Dec 1976).

APPARATUS

The data for this analysis were acquired in October 1976 using the DTNSRDC Carriage III high-speed towing facility operated by the Experimental Aero-Hydro Group of the Aviation and Surface Effects Department. The useable dimensions of the tow basin are 2,110 ft (643.1 m) long, 20 ft (6.1 m) wide, and 10 to 16 ft (3.0 to 4.9 m) deep. The wavemaker, located at the east end of the tow basin, is a pneumatic type which produces waves by cyclical variation of air pressure on the water surface. Irregular head waves were produced to approximate 1/30-scale Pierson-Moskowitz spectra for fully arisen Sea States 4 and 5 with significant wave heights (H 1/3) of 2.76 and 4.00 in. (7.01 and 10.16 cm).

The model was designed to attach to the carriage by an aluminum block clamped to the pipe at wing midspan. The block was bolted to a 2-in. (5.1-cm) block gage for drag measurement relative to the tow post of the carriage. Unloader springs attached to the tow post were used to adjust the model to the desired nominal weight of 88.5 lb (40.1 kg). The resultant arrangement gave a model free in heave, fixed in pitch, and fixed in roll. (The analyzed data represent only zero pitch and roll.) Additional data were taken from heave position, propulsor fan rpm, and center-of-gravity acceleration. The general arrangement of the PAR-WIG model on the carriage support system is shown in Figure 1.

MODEL

The PAR-WIG model contains five major components that can be parametrically varied. Of these components, the wing, fuselages, and propulsor fans remained fixed throughout the evaluation. The wing flap and endplates (all components extending below the wing bottom) were studied for load alleviation. The general arrangement of the model is illustrated in Figure 2.

The wing portion of the model is a NACA 0015 thickness distribution, cambered to produce a straight bottom surface from the leading edge radius back to the trailing edge. The wing has an aspect ratio of 1 with a span and a total chord (wing portion plus flap) of 48 in. (1.22 m).

The two fuselages are square tubes angled upward at an attitude of two degrees with respect to the wing bottom surface. The forward ends of the fuselages are faired with pentahedral inserts.

Two propulsor fans symmetrically arranged on each fuselage give a total of four fans. The fans are angled to produce a thrust vector which is 20 deg upward from the mean waterline.

Two distinct types of wing flaps were used. The first type, a rigid flap, is merely the aft 0.21 chord of the airfoil section pivoted 40 deg downward at the bottom surface. The second type, a flexible flap, is a load alleviation device which represents one of the concepts investigated. This flexible flap consists of the main rigid flap deflected 20 deg plus a light, split flap which can deflect an additional 20 deg. The deflection of the split flap is controlled by a low pressure air bag between the main and split flaps. The air in the bag is supplied by an electric fan, and the pressure is controlled by adjustable vents. Air pressure listed for this flap is nominal and should be noted in any comparisons throughout this analysis. Figure 3 shows both the rigid and flexible flap with the rigid portion fixed at zero angle for illustration purpose only.

An endplate is attached at each end of the wing portion, and Figure 4 illustrates the four types of endplates used. The basic rigid endplate is made of fiberglass with a flat-faced forebody planing surface of wood as shown in Figure 5a. The second type endplate is also the second load alleviation device investigated. This endplate, entitled bumpers/springs, is the basic rigid endplate with the wooden planing surface spring-mounted as a wave impact bumper on either two or four internal springs. Although the external appearance of these endplates is identical,

the internal difference is illustrated in Figure 5b by showing a spring for each of the four stiffnesses evaluated. The soft endplate (formally referenced as the flexible endplate) is the third type endplate and the third load alleviation device investigated. This endplate is basically an air-filled plenum with 61 flexible nylon fingers along the lower edge as shown in Figure 5c. Due to the material thickness used, the fingers had a certain excess rigidity even when unpressurized. Figure 5d shows the metal endplate made from a 0.25-in. (6.35-mm) solid aluminum plate; this endplate is included only for comparison purposes. It should be noted that height d for the four endplates varies from 6.89 to 7.75 in. (17.5 to 20.0 cm), and this height should be remembered when making average heave comparisons. A more complete list of information for the model components is given in Table 1.

DATA REDUCTION

Data acquisition in Sea State 0 (calm water) was straightforward because it was relatively easy to establish mean values for parameters such as heave and drag. The procedure was to have the computer calculate the time average for data acquired along 100 ft (30.5 m) of tow tank encounter length.

Data acquisition during irregular head waves was more complex than calm water data acquisition. For waves, it became necessary to statistically compute data values such as heave, drag, and acceleration. (A wave set is the total series of waves that represent the desired spectra resulting from a given wavemaker generation. The wave set is terminated when appreciable degradation occurs from tow-tank wave reflections and residual model disturbances.) Statistically, the best representation for a given data value is to acquire ample data for a given wave set as well as for additional wave sets. In this way a more representative value for a significant wave height can be obtained. Significant wave height can vary along the tow tank length as well as with time in a given wave set in addition to the variation for distinct

wave sets. However, limitations on resources requires a limited data sample. With this in mind, a single data value for Sea States 4 or 5 represents a sample of information acquired for approximately 100 wave encounters of a given single wave set.

Prior to this investigation, a propulsor fan calibration was performed to determine thrust output. The procedure was to calibrate fan thrust versus fan rotational velocity and carriage velocity in the following manner. Two fans with nacelles were mounted horizontally on a dynamometer via a faired strut. With the fans suspended approximately 15 in. (38 cm) above the mean waterline, a series of turbine tip drive pressures were then tested over the range of carriage velocities desired. The resultant family of carriage velocity curves for thrust versus fan rotational velocity provided the installed propulsor thrust for this investigation.

Model average drag was calculated from the output of a block gage and the thrust calibration. The time average for a given carriage velocity and wave set was computed by:

$$\text{Drag} = \text{Gage} + \text{Thrust}_{\text{Speed}} \cdot \text{Cos}\ \theta_F$$

where the thrust was corrected for carriage velocity and fan angle. Model average heave was calculated from the time average output of the heave potentiometer computed from a given carriage velocity and wave set. The resultant heave value is the mean distance of the wing lower surface (positive above) from the mean waterline. Rms values were computed for the vertical acceleration of the model center of gravity and the heave position. Rms represents the square root of the average squared data value for a given carriage velocity and wave set. Single sample accuracy for the data items of interest is given in Table 2.

EFFECT OF PRESSURE VARIATION IN FLEXIBLE FLAP

Based on the available data, the pressure effect in the flexible air-bag flap was investigated. The model was configured with the metal endplates and with the 40-deg flexible flap. Figure 6 shows the 0.25 thrust-to-weight ratio data plotted for the Sea State 5 condition. Included for reference only are the cases of 0 and 3 lb/ft^2 (0 and 14.6 kg/m^2), since it is necessary to have a pressure greater than the wing loading of 5.5 lb/ft^2 (26.85 kg/m^2) to prevent the air bag from collapsing against the 20-deg rigid flap portion. For the 7- and 12-lb/ft^2 (34.2- and 58.6-kg/m^2) data, increasing average pressure in the air bag had the effect of increasing the average heave and drag over the lower velocities to 15 ft/sec (16.5 km/hr). None of the pressures investigated had much effect on the ride quality (rms acceleration) or wave following (rms heave) of the ride throughout the velocity range.

EFFECTIVENESS OF FLEXIBLE FLAP

The flexible air-bag flap was compared for effectiveness to the rigid flap under the same conditions up to a velocity of 15 ft/sec (16.5 km/hr). The model was configured with the metal endplates to isolate flap effect and with a nominal flap pressure of 11 lb/ft^2 (53.7 kg/m^2). The combination of a thrust-to-weight ratio of 0.20, a Sea State 5, and both flaps at the 40-deg total angle setting gave conditions of lower heave position for maximum flap effect. Figure 7 shows a smoother ride (rms acceleration and rms heave) at the expense of decreased average heave and increased average drag for the flexible flap.

EFFECT OF SEA STATE ON MODEL WITHOUT LOAD ALLEVIATION

As reference information, the effect of various sea states on the model configured with metal endplates and 40-deg rigid flap was investigated and is presented as Figure 8. The nominal thrust-to-weight ratio was 0.20 in Sea States 0 and 5. Note that this configuration in Sea State 5 was used in the flap evaluation of Figure 7. Figure 8 shows

a higher average heave for the higher sea state throughout the velocity range. The endplates actually clear the average waterline at velocities greater than 12 and 15 ft/sec (13.2 and 16.5 km/hr) for Sea States 5 and 0. The average drag for both sea states is approximately the same throughout the velocity range. Rms acceleration for Sea State 5 increased from 0.030 to 0.100 G's for velocities of 0 to 15 ft/sec (0 to 16.5 km/hr); rms acceleration was constant for the remainder of the velocity range. Rms heave values indicated only a slight wave following at velocities below 15 ft/sec (16.5 km/hr); whereas, higher velocities indicated an obvious wave cut through for a nonresponsive condition. Rms acceleration and rms heave are assigned values of zero for Sea State 0.

A good assessment of sea state effect can be determined from the transport efficiency η_T of the model at cruise condition. Since all data were taken for accelerating flight with excess thrust, the cruise velocity is determined by extrapolating excess thrust to zero as shown in Figure 8. The extrapolation uses data for velocities above 10 ft/sec (11 km/hr) to avoid any "hump" phenomenon. Total thrust, which just offsets total drag, is determined from the propulsor fan calibration. The ducted-fan propulsor jet velocity V_j is calculated by solving the quadratic equation:

$$T = \rho A_j V_j (V_j - V)$$

Total propulsive power is then calculated from the formulation:

$$P = \rho A_j V_j (V_j^2/2 - V^2/2)$$

Transport efficiency η_T is readily calculated since $\eta_T = WV/P$. The resultant η_T for the model without load alleviation calculates as 23.18 for Sea State 0 with a degradation to 10.06 for Sea State 5. The degradation is large because of the efficient condition with the endplates just clear of the average waterline for Sea State 0 as shown on the average heave plot of Figure 8. The L/D also degraded from 27.41 to 13.66 for increase in sea state. A synoptic presentation of the main values of the calculations are given in Table 3.

EFFECT OF PRESSURE VARIATION IN SOFT ENDPLATES

The effect of varying the average pressure in the flexible fingers of the soft endplates was investigated for a thrust-to-weight ratio of 0.25 in Sea State 5 conditions. Figure 9 presents all available data for these conditions with the rigid flap at the 40-deg position. Changing pressure from 0 to 1.0 lb/in.^{2}(0 to 703.1 kg/m^2) seemed to have very little effect on average heave, ride quality (rms acceleration), and wave following (rms heave) for the velocity conditions available. Note that most pressures were investigated at only 0- and 35-ft/sec (0- and 38.4-km/hr) conditions. A mechanism design flaw may be responsible for the average drag increment across the velocity range. At forward velocities in Sea State 5, the combination of PAR effect and wave impact forced the bow finger laterally outward and backward to partially wrap around the second finger. The consequent average drag tends to be a function of the amount the single finger wraps backward and protrudes into the waves. The laterally protruding finger, which is more rigid, would therefore present a larger area to the waves with an increase in average drag.

EFFECT OF SEA STATE ON SOFT ENDPLATES

The effect of various sea states on the model with soft endplates and 40-deg rigid flap is shown in Figure 10. Sea States 0, 4, and 5 were used to evaluate the endplates with fingers inflated to a nominal 0.50 lb/in.^{2} (352 kg/m^2). The thrust-to-weight ratio was maintained at 0.25. Although average heave for Sea States 0 and 4 is essentially the same across the velocity range, Sea State 5 shows an increase. The same trends are shown for average drag. Remembering that rms acceleration and rms heave for Sea State 0 are assigned zero values, Sea State 5 is approximately twice as rough riding (rms acceleration) as Sea State 4 across the velocity range. The worst conditions exist at 15 ft/sec (16.5 km/hr) where the ride qualities (rms accelerations) level out for the higher velocities. Rms heave shows an appreciable decrease in wave

following with increase in velocity which indicates the endplates begin to cut through the waves. With increasing velocity the wave following (rms heave) varies from three to two times greater for Sea State 5 than for Sea State 4. Note that these soft endplates have more drag with a rougher ride than the metal endplates without the load alleviation of Figure 8.

EFFECT OF THRUST-TO-WEIGHT RATIO ON SOFT ENDPLATES

The effect of two thrust-to-weight ratios (0.20 and 0.25) on the model configured with the soft endplates is shown in Figure 11. The endplates were inflated to a nominal pressure of 0.50 lb/in.^{2} (352 kg/m^2), and the rigid flaps were positioned to the 40-deg setting. The more severe cases, which are at Sea State 5, are presented to illustrate maximum effect. It is obvious from average heave that the lower thrust-to-weight ratio would not fly (support the model weight with PAR only) at zero velocity. At all other velocities the lower 0.20 thrust-to-weight ratio remained lower than the 0.25 ratio by more than 1 in. (2.54 cm). It appears that for velocities less than 13 ft/sec (14.3 km/hr), the 6.89-in. (17.50-cm) endplates are below the mean waterline for the 0.20 condition. Average drag shows a resultant drag penalty of at least 2 lb (0.91 kg) across the velocity range for the lower thrust-to-weight ratio. The ride quality comparison is not as clear because the lower thrust-to-weight ratio increases in rms acceleration with increasing velocity; whereas, the higher thrust-to-weight ratio starts higher and levels off lower at the midvelocity range. The rms heave comparison partially explains the ride quality as the lower thrust-to-weight ratio tends to follow the wave motion across the velocity range. The net result would be an increasingly rougher ride with increased velocity. In contrast, the higher thrust-to-weight ratio with the least interface tends to follow the waves at low velocities; whereas, at the higher velocities the endplates cut through the waves.

EFFECTIVENESS OF SOFT ENDPLATES

The effectivenss of the soft endplates was investigated by comparing them to the similar sized basic rigid endplates under the same conditions. Figure 12 shows the maximum effect which is at Sea State 5 conditions. The soft endplates are presented for inflation pressures of 0.25 and 0.50 lb/in^2 (176 and 352 kg/m^2); these cases show the most data scatter. Two sets of repeat data for the velocity range are presented for the basic rigid endplates. All models were configured with the rigid flap at the 40-deg setting and with the thrust-to-weight ratio of 0.25. Although average heave shows no apparent difference with velocity for the three configurations, it must be remembered that the basic rigid endplates are 0.23 in. (5.8 mm) deeper with respect to the wing lower surface than the soft endplates. As a result, average heave indicates a loss of PAR beneath the endplates to be significant. The most noticable difference in average drag with velocity is shown for the two soft endplate pressures discussed in the previous section on inflation pressure effects. Realistically, the conclusion is that no average drag increment exists because of the design mechanism which allowed bow-finger lateral movement. No decisive conclusion can be drawn about ride quality except for a slight reduction in rms acceleration for the soft endplates at the higher velocities. Rms heave shows the same type of trends in that the soft endplates tend to do less wave following at the higher velocities.

EFFECT OF SPRING STIFFNESS ON BUMPERS/SPRINGS ENDPLATES

The effect of varying the spring stiffness behind the sprung fore-body planing surfaces was investigated for the bumpers/springs endplates. Conditions were set for a thrust-to-weight ratio of 0.25 and Sea State of 5. The model was configured with the rigid flap set to the 40-deg position.

To eliminate possible mechanism effects, the data presented are restricted to bumpers with two springs. A total of five spring stiffnesses were investigated (See Figure 13) as follows:

Springs	Compression Force (Per Spring) lb/in.	(kg/cm)
2	26	(4.6)
2	54	(9.6)
2	78	(13.9)
2	102	(18.2)
0 (Basic rigid)	∞	(∞)

The basic rigid endplate is included for comparison because it is an infinite rigidity spring. Due to time constraints, three stiffnesses were investigated for velocities of only 0 and 25 ft/sec (0 and 27.4 km/hr).

The average heave with respect to velocity shows no appreciable difference for the various spring stiffnesses. However, average drag shows an unexplained difference for the two stiffnesses of 54 and 78 lb/in. (9.6 and 13.9 kg/cm). Close inspection of other related data such as significant wave height, total wave encounter, and block-gage sensitivity revealed nothing to justify a discrepancy of this magnitude. Neither rms acceleration nor rms heave shows any apparent effect for the various two-spring stiffnesses throughout the velocity range.

EFFECTIVENESS OF BUMPERS/SPRINGS ENDPLATES

The effectiveness of the bumper-endplate mechanism can be determined by comparing the bumpers/springs endplates to the basic rigid endplates. This comparison is shown in the data of Figure 13. Conditions were again set for a thrust-to-weight ratio of 0.25 and Sea State of 5, and the model was configured with the rigid flap set to the 40-deg position.

Discussion of average heave, average drag, rms acceleration, and rms heave apply as stated in the prior section on spring stiffness.

In summary, the only effect indicated by the presented data is an unexplained increment in average drag. During the tow tank investigation, the bumper was observed to be moving when encountering waves similar to an automobile undercarriage when encountering road surface irregularities. Since the automobile passenger feels only an attenuated bounce, the bumpered endplate should also alleviate high-wave impacts for a properly designed mass and mechanism. The complete data set seems to indicate that further investigation in terms of mechanism design and/or data type may be required to properly evaluate the bumpered endplate concept. Mechanism redesign may require energy absorption by means other than springs which can permit misalignment with the present mechanism. Analysis of other data types, such as impact acceleration, fatigue life, and oblique waves, may also be required to evaluate the concept.

EFFECT OF SEA STATE ON BASIC RIGID ENDPLATES

The effect of sea state variation on the model configured with the basic rigid endplates and 40-deg rigid flap was investigated for a thrust-to-weight ratio of 0.25. Figure 14 shows data for Sea States 0, 4, and 5. For Sea States 0 and 4, average heave increases with sea state, and the total increment increases with velocity. Average heave for Sea State 5 is lower than or equal to heave in the two other sea states. Whereas average drag versus velocity is identical for Sea States 0 and 4, average drag for Sea State 5 is approximately 1 lb (0.45 kg) less than for the other sea states, except at 35 ft/sec (38.4 km/hr) where the opposite is true. Understandably, rms acceleration (ride quality) increased with sea state and velocity. Rms heave shows wave following to be high for the high sea states and low velocities which indicates model ability to respond to the slow approach of waves. For velocities greater than 25 ft/sec (27.4 km/hr), rms heave is constant which indicates the model must cut through the oncoming waves. Note that rms acceleration and rms heave are assigned values of zero for Sea State 0.

EFFECT OF THRUST-TO-WEIGHT RATIO ON BASIC RIGID ENDPLATES

The effect of thrust-to-weight ratio variation was investigated for the model configured with the basic rigid endplates and the 40-deg rigid flap. Available data allowed comparisons to be made for thrust-to-weight ratios of 0.20 and 0.25 at only the Sea State 0 condition. Figure 15 shows an increase in average heave of approximately 1 in. (2.54 cm) for the higher 0.25 thrust-to-weight ratio throughout the complete velocity range. However, average drag is identical for both ratios up to 9 ft/sec (9.9 km/hr) where the 0.20 thrust-to-weight ratio drag increment increases with velocity to about 1 lb (0.45 kg) at 35 ft/sec (38.4 km/hr).

CONCLUSIONS

A PAR-WIG parametric model was investigated at DTNSRDC to provide a data base which can be used for evaluating the effectiveness of some load alleviation devices. Soft and bumpered endplates and a flexible flap were evaluated for irregular head Sea States 0, 4, and 5 through a velocity range from 0 to 35 ft/sec (0 to 38.4 km/hr). In contrast, the model without load alleviation devices was evaluated under identical conditions.

The following conclusions can be drawn from the results of this investigation:

1. Data available for velocities up to 15 ft/sec (16.5 km/hr) indicate the flexible flap concept can provide a smoother, softer ride for a thrust-to-weight ratio of 0.20 but at the expense of decreased average heave and increased average drag.

2. Pressure variation in the soft endplates has no effect on either average heave and drag or rms acceleration (C.G.) and heave. This conclusion needs qualification as an average drag increment exists for different endplate pressures. The increment is probably due to a faulty

design which permits excessive lateral movement of the bow fingers of the endplates.

3. The soft endplates have no significant improvement over the basic rigid endplates with regard to either average heave and drag or rms acceleration (C.G.) and heave. This conclusion needs qualification for the excess material stiffness used in the fingers of the soft endplates.

4. For the various spring stiffnesses investigated, the bumpers/springs endplate results show no effect on average heave, rms heave, and rms acceleration.

5. The implementation of the soft endplate concept requires an endplate width that results in a rougher ride with more drag than the narrow, metal endplates.

6. On the model without load alleviation, transport efficiency decreases from 23.18 to 10.06 with increase in Sea State from 0 to 5.

RECOMMENDATIONS

Because of the anticipated potential of both the soft and bumpered endplate concepts, further exploration is recommended; however, the design of the endplate must be optimized. For example, a thin, soft material should be used for a narrow, soft endplate design that does not permit bow finger lateral bending. The bumpered design should have a scaled bumper mass that cannot misalign on impact. In addition, studies should include additional types of data such as impact acceleration, fatigue lift, and oblique waves.

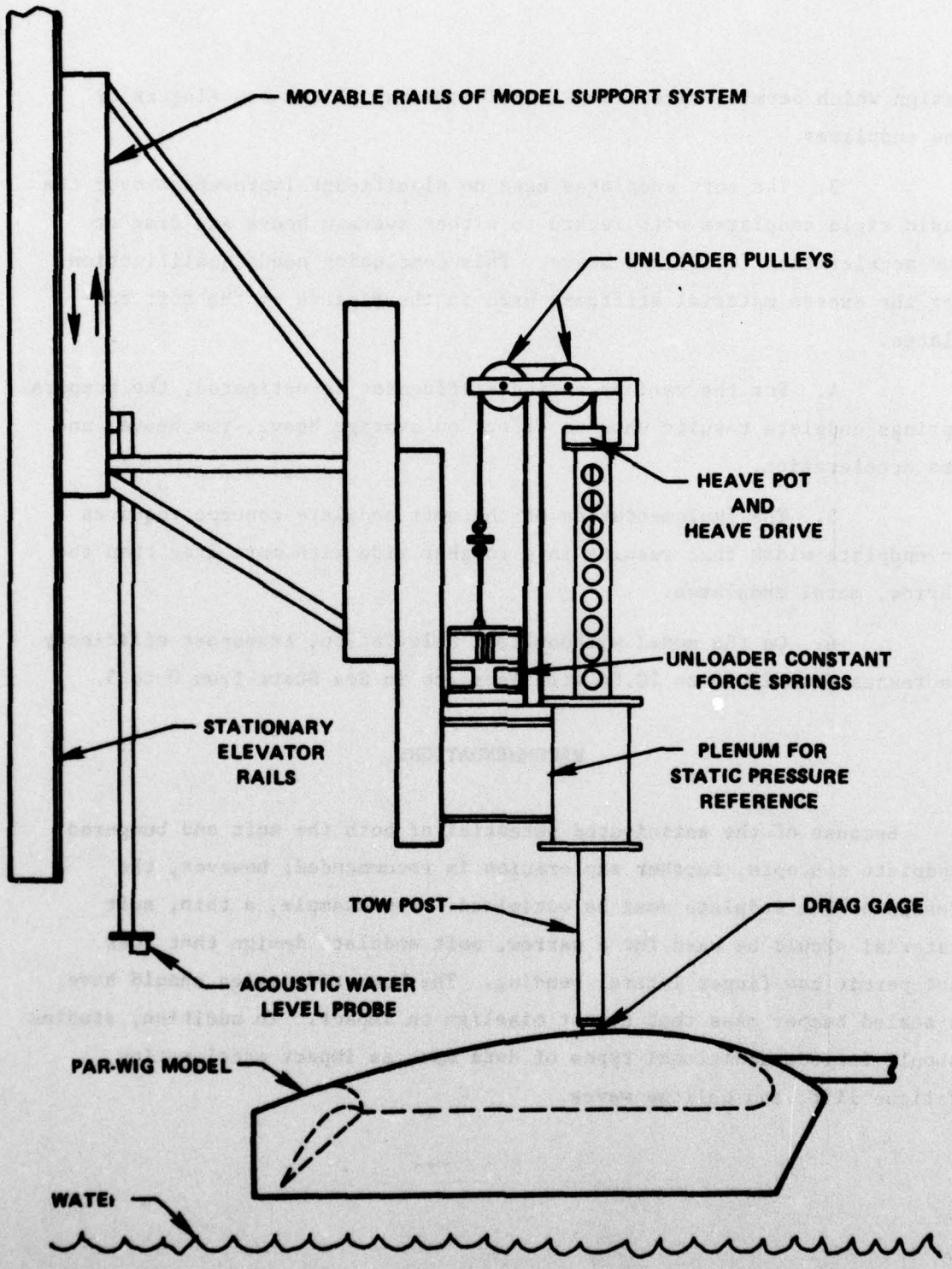

Figure 1 - PAR-WIG Model on Carriage III Support System

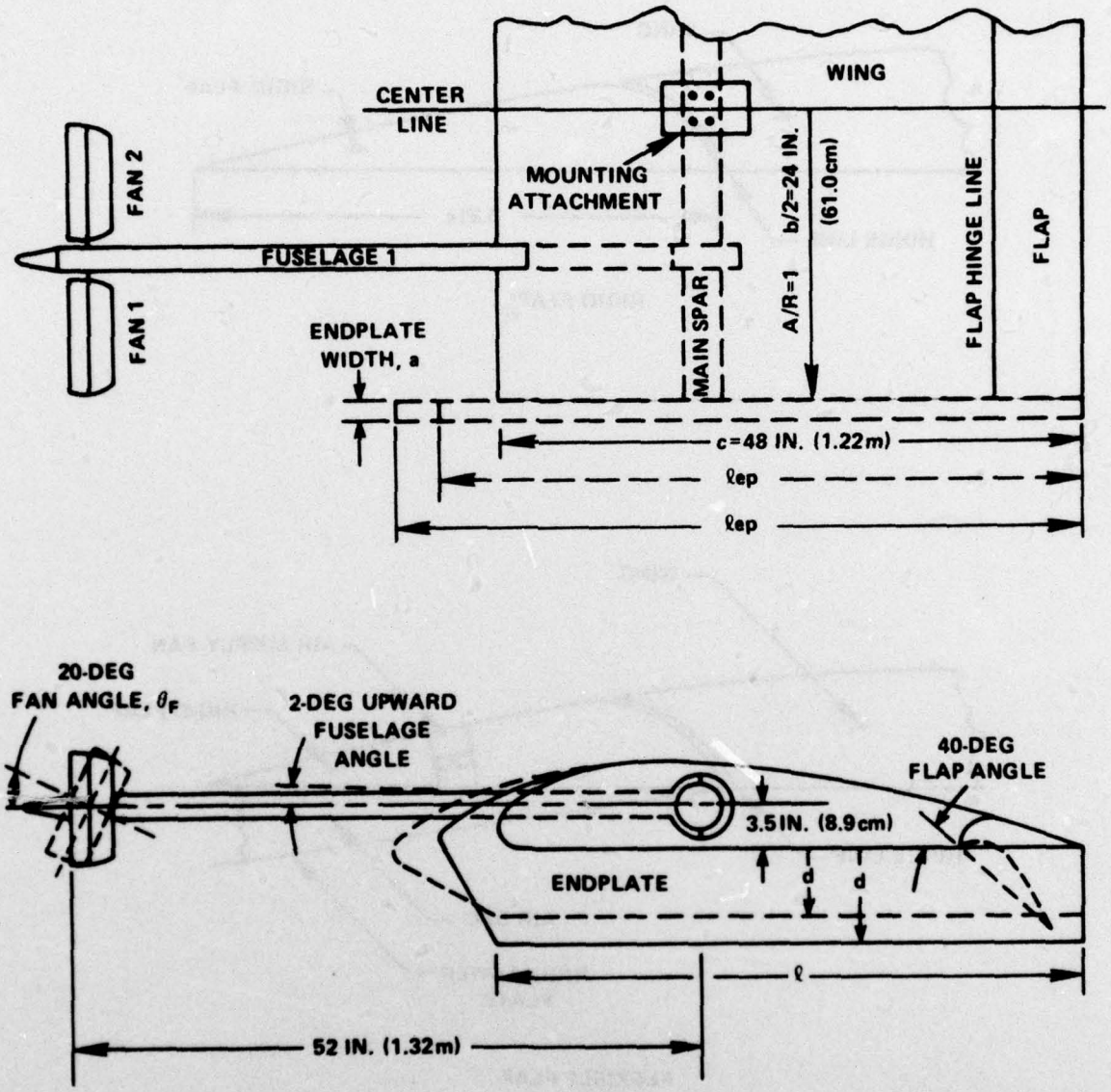

Figure 2 - General Arrangement of PAR-WIG Model

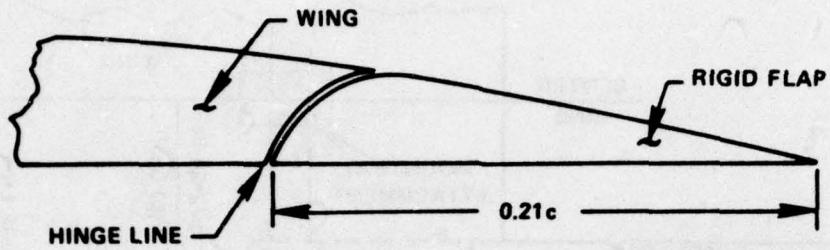

RIGID FLAP

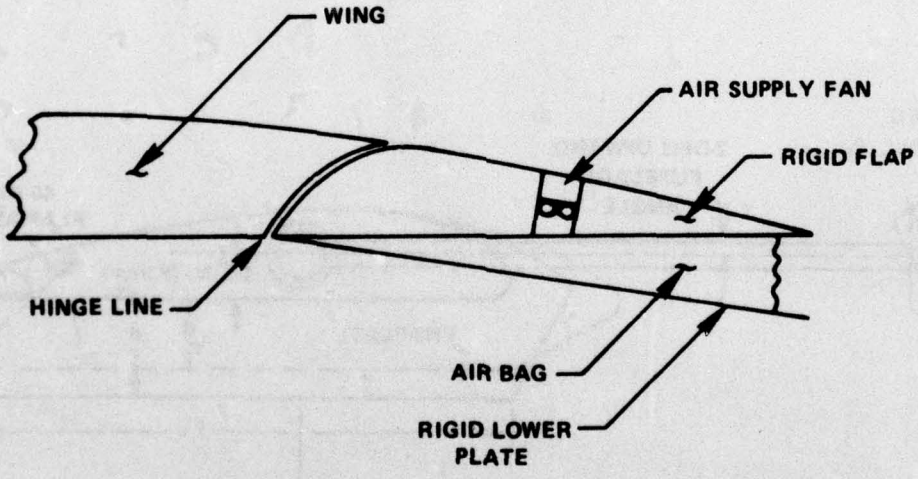

FLEXIBLE FLAP

Figure 3 - Model Flap Configurations

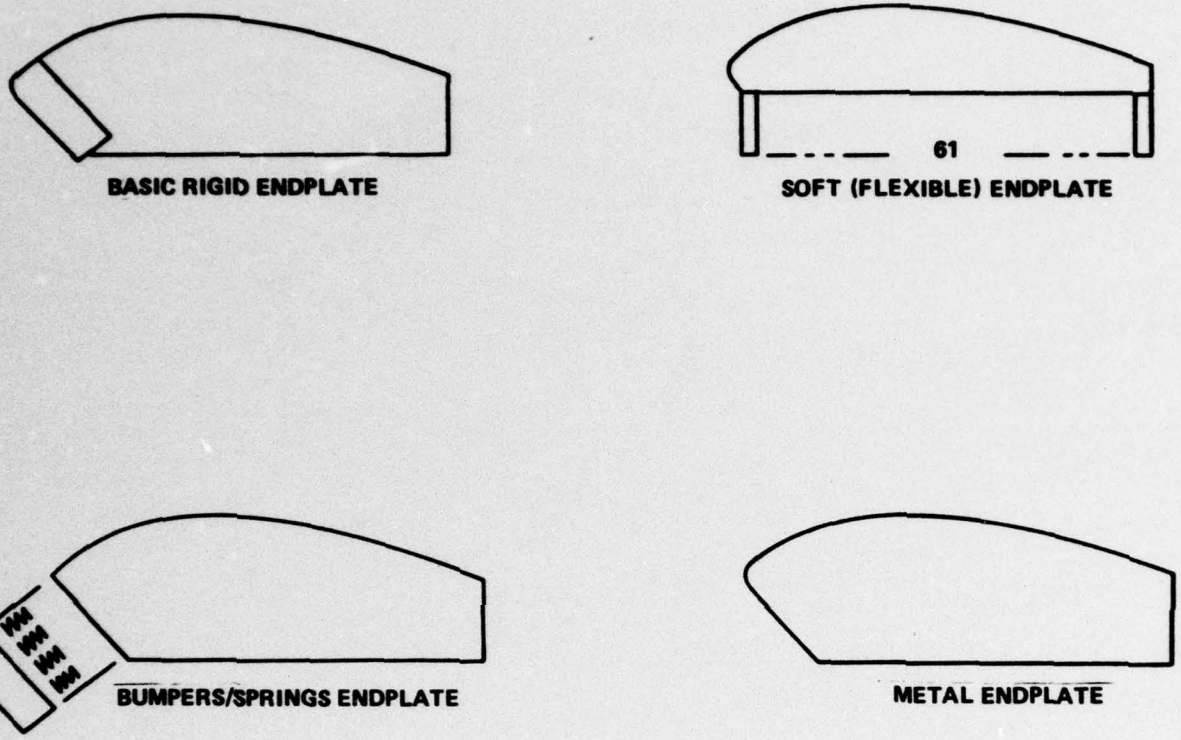

Figure 4 - Model Endplate Configurations

Figure 5 - Endplates Removed from Model

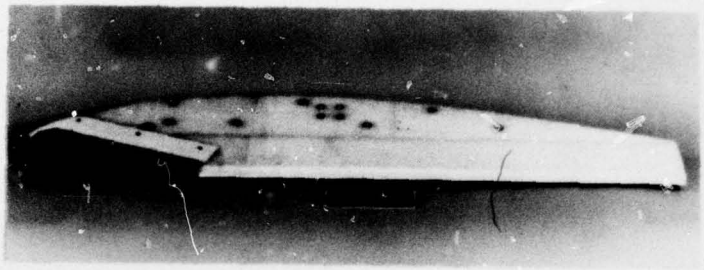

Figure 5a - Basic Rigid Endplate

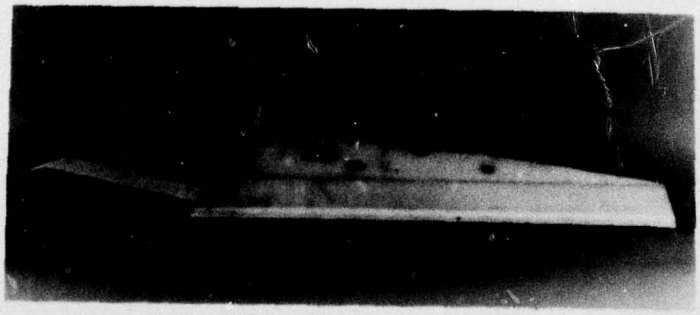

Figure 5b - Bumpers/Springs Endplate

Figure 5c - Soft (Flexible) Endplate

Figure 5d - Metal Endplate

Figure 6 - Flexible Flap Pressures for T/W = 0.25 at Sea State 5

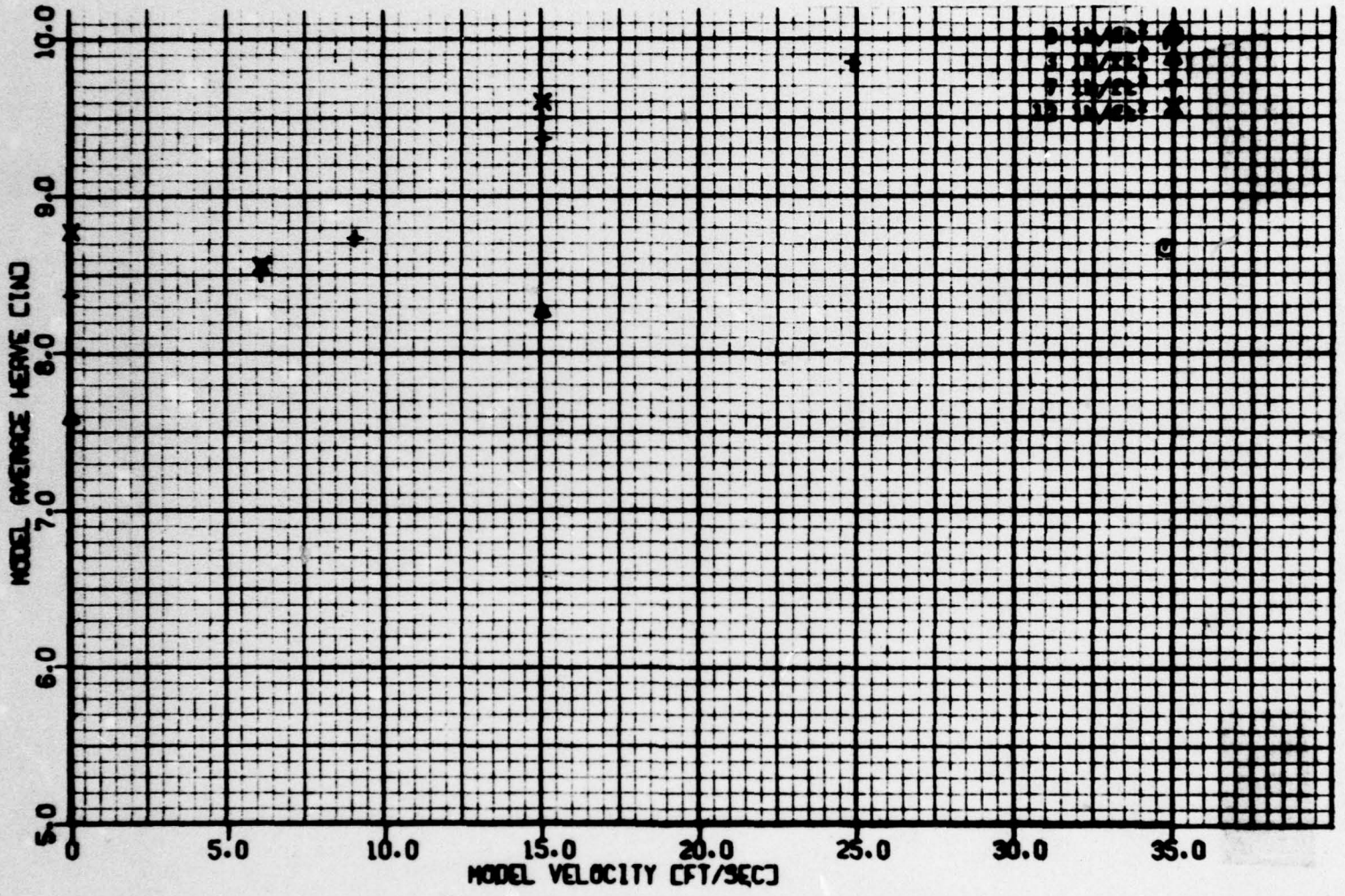

Figure 6a - Model Average Heave Versus Model Velocity

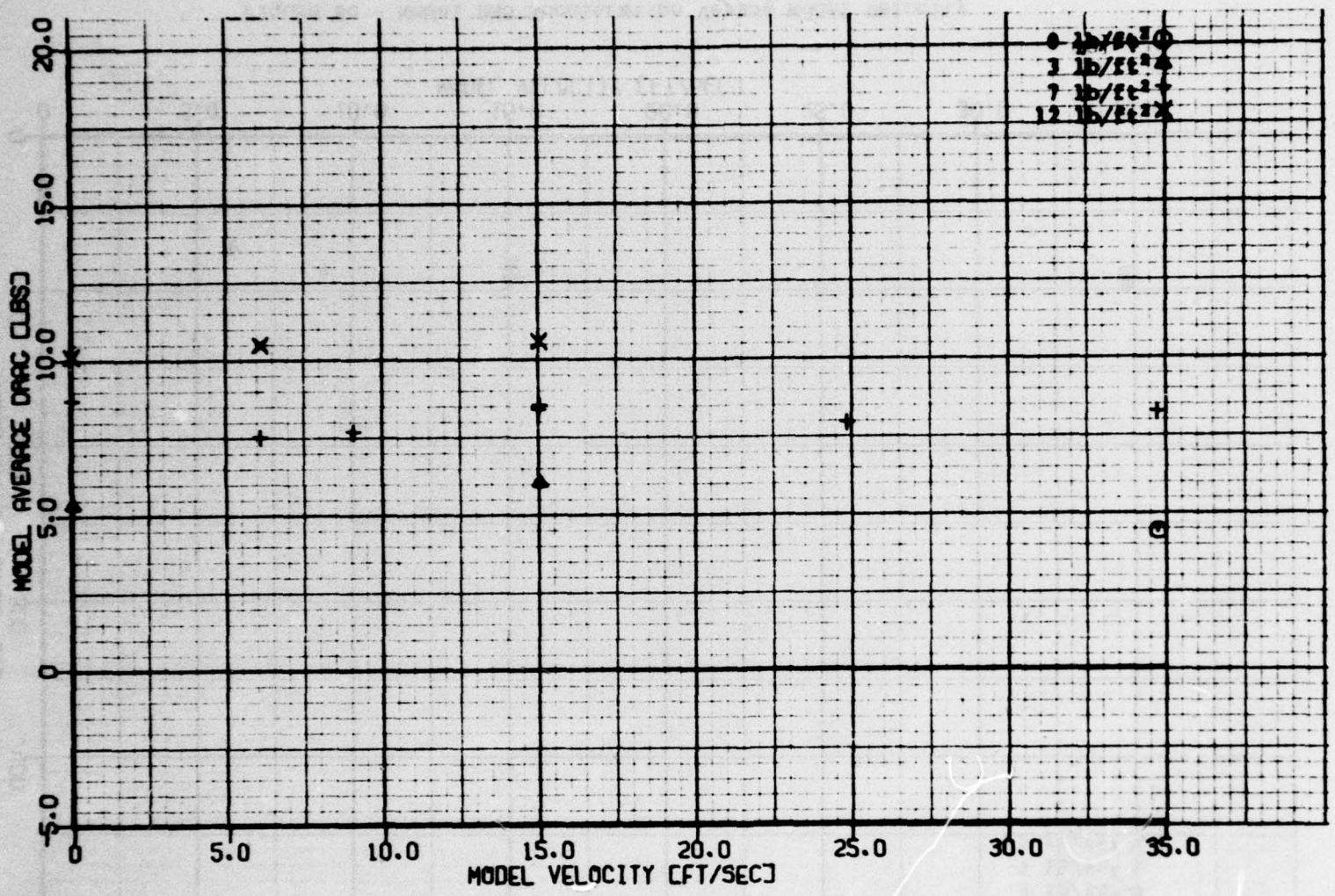

Figure 6b - Model Average Drag Versus Model Velocity

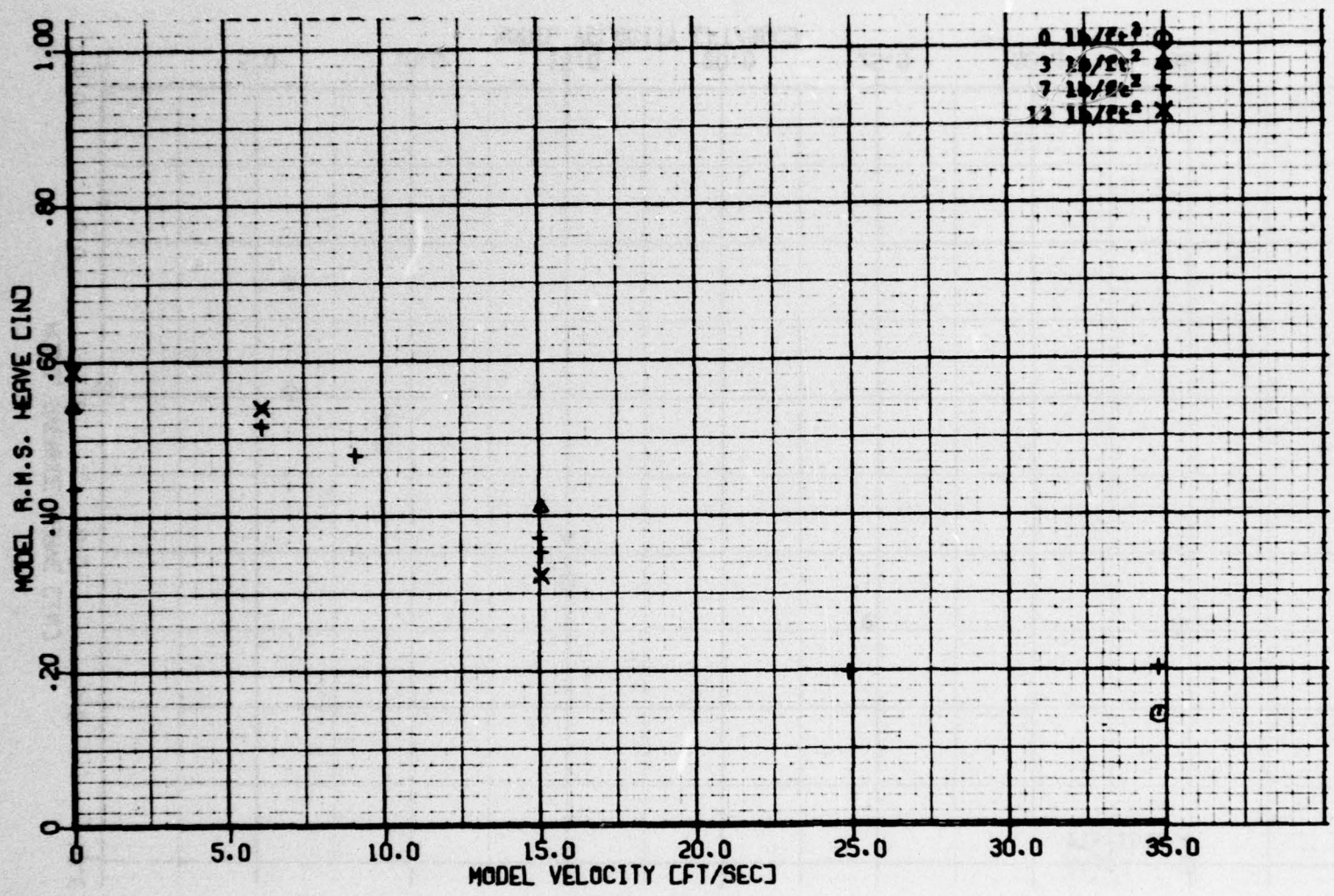

Figure 6d - Model RMS Heave Versus Model Velocity

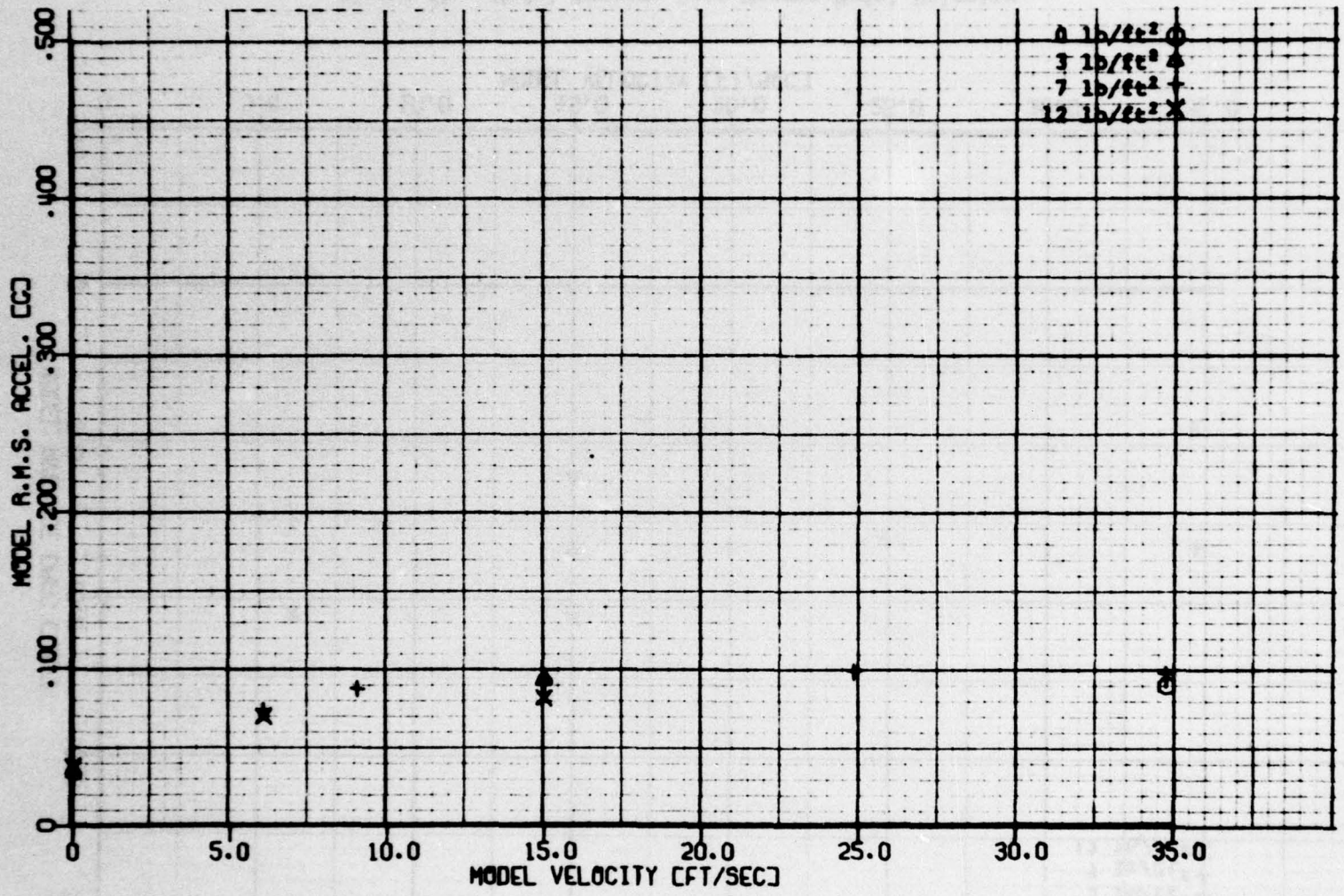

Figure 6c - Model RMS Acceleration Versus Model Velocity

Figure 7 - Rigid Versus Flexible Flap for T/W = 0.20 at Sea State 5

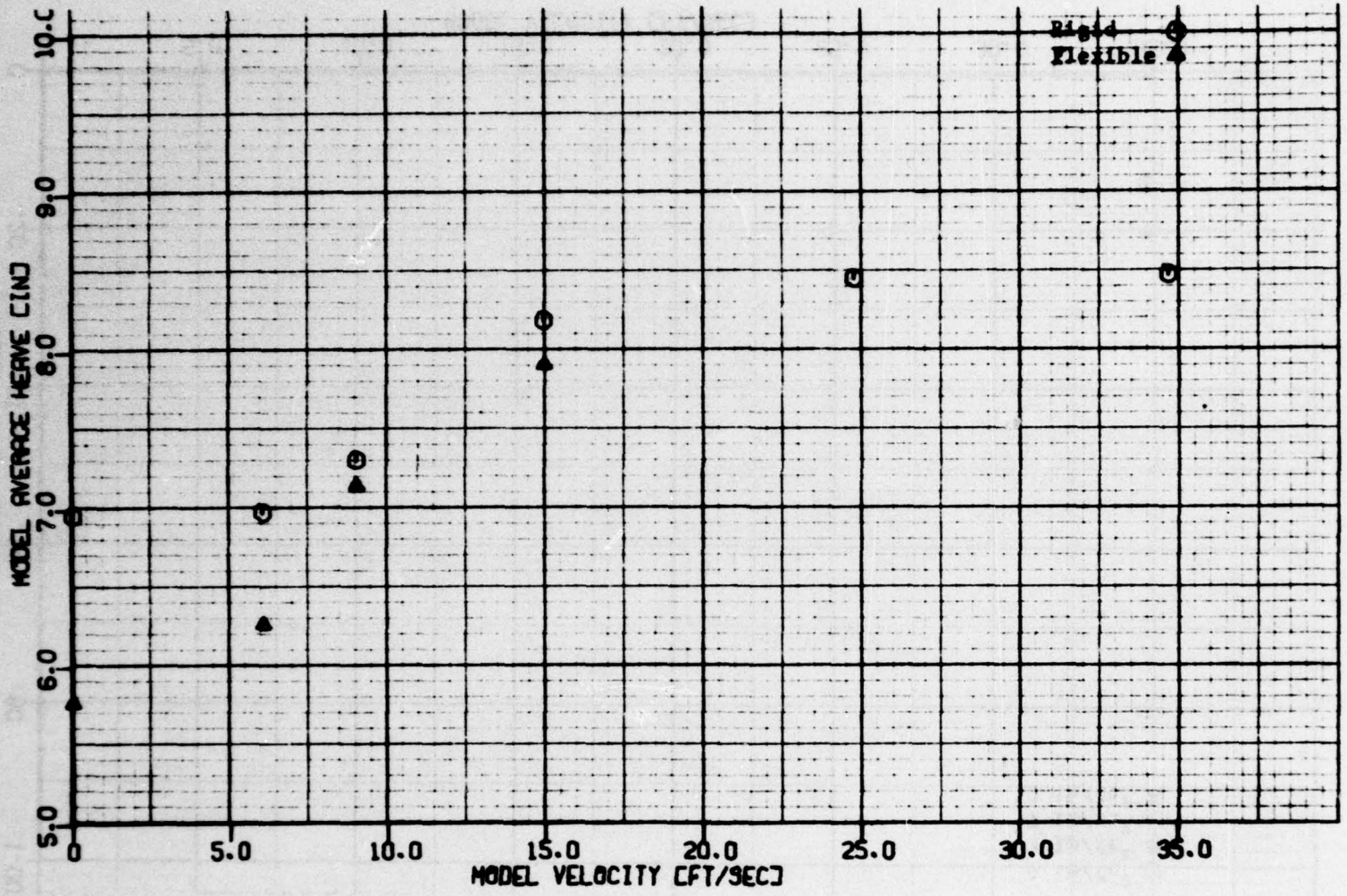

Figure 7a - Model Average Heave Versus Model Velocity

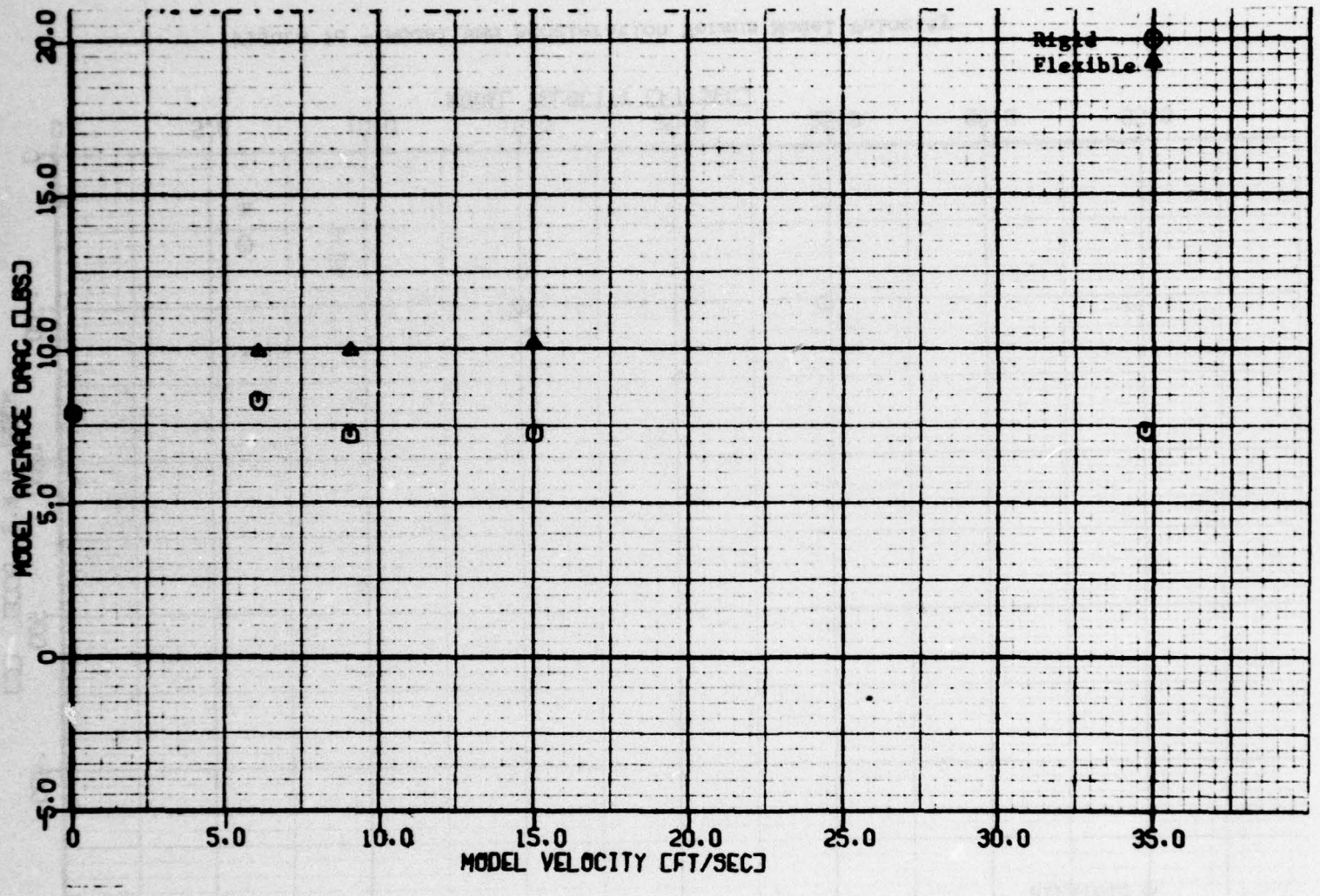

Figure 7b - Model Average Drag Versus Model Velocity

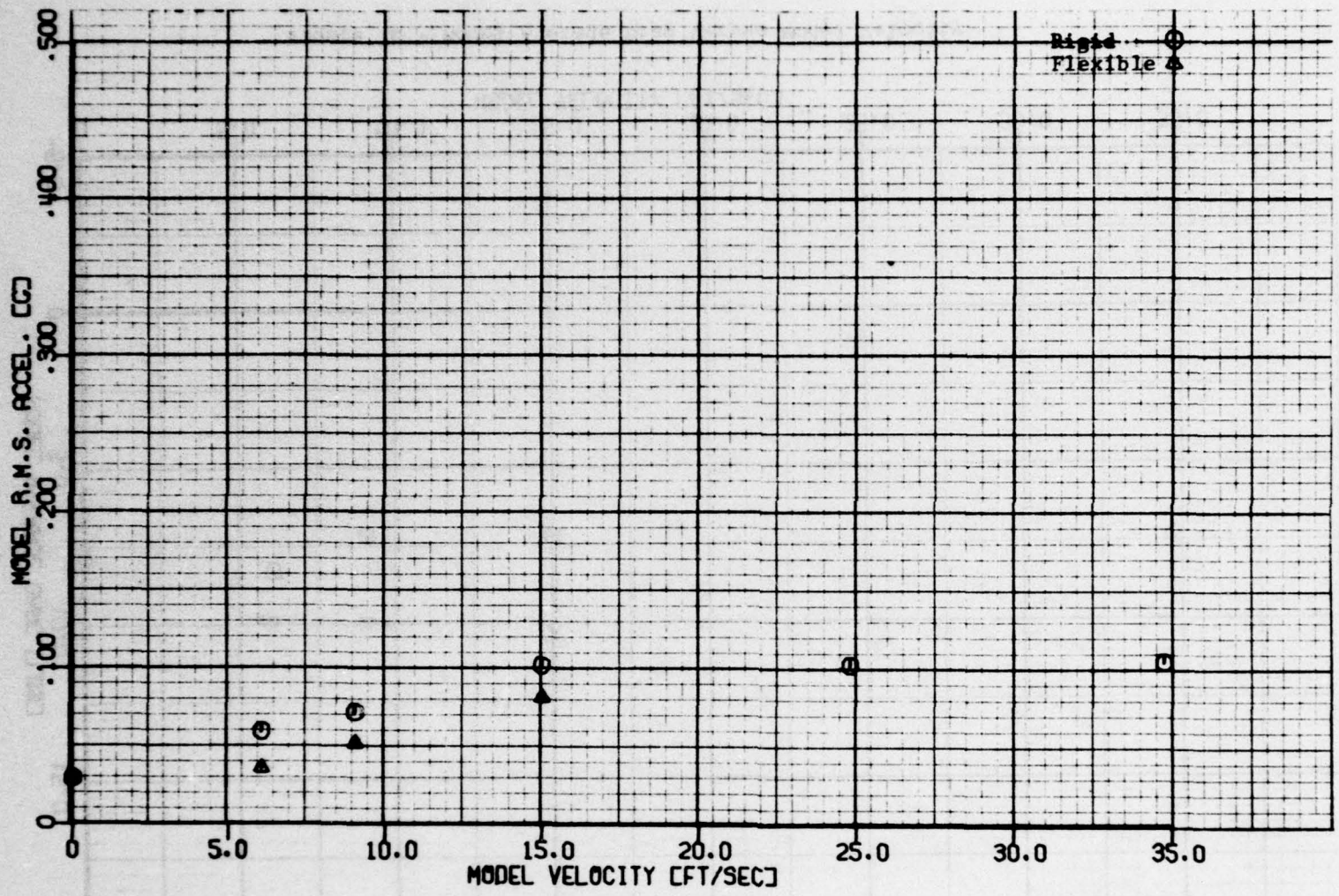

Figure 7c - Model RMS Acceleration Versus Model Velocity

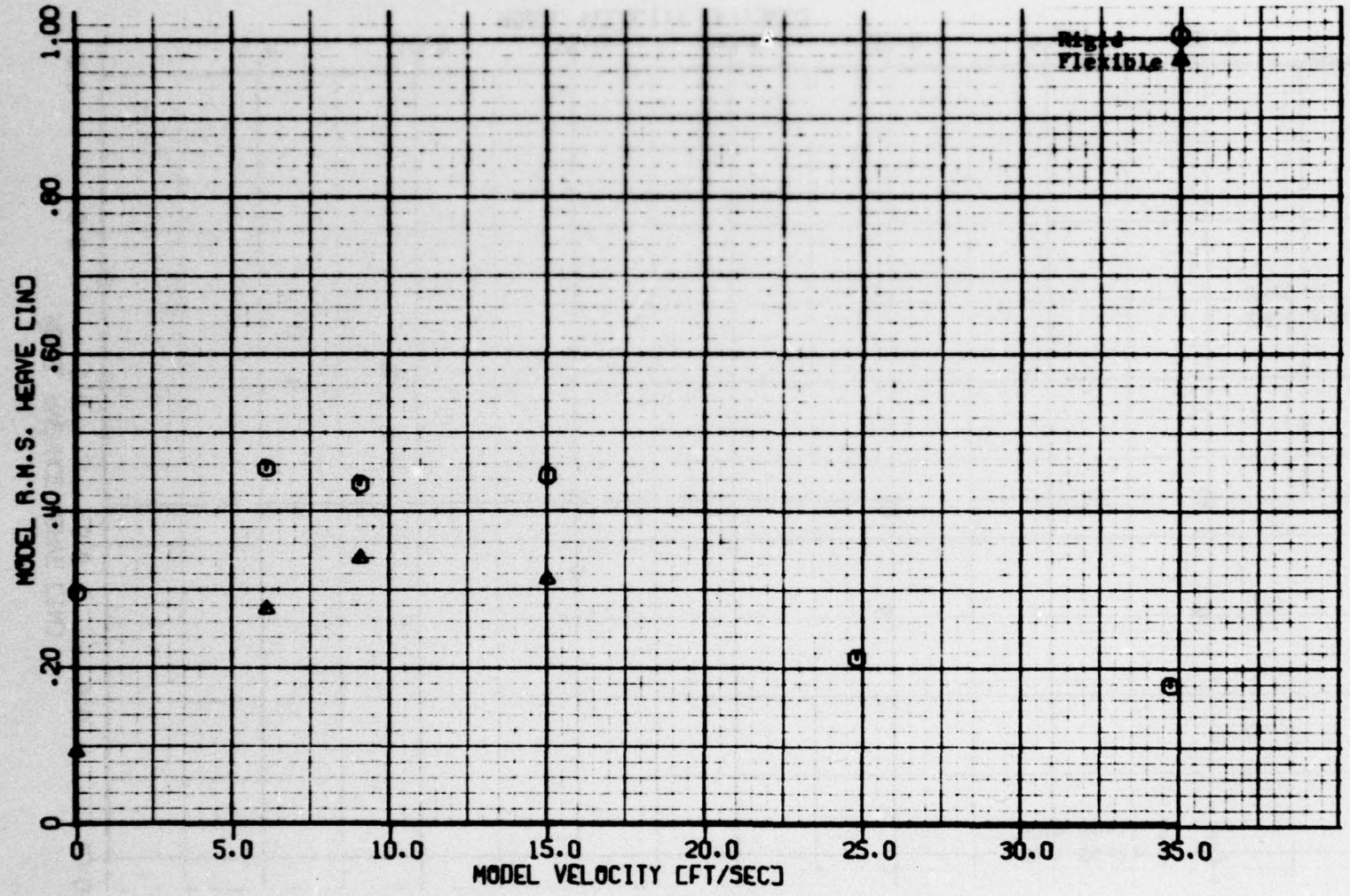

Figure 7d - Model RMS Heave Versus Model Velocity

Figure 8 - Metal Endplate with Rigid Flap for T/W = 0.20 at Sea States 0 and 5

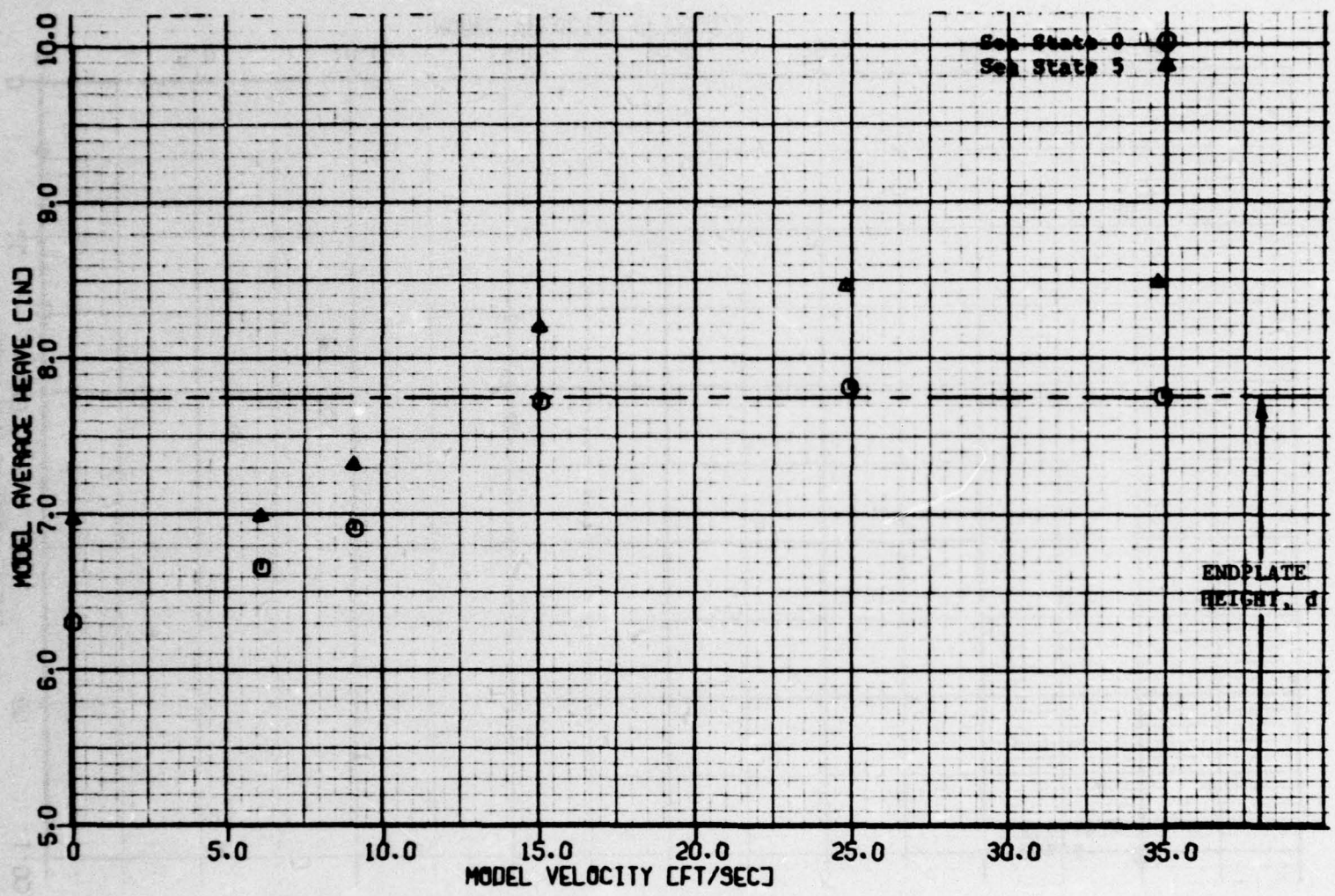

Figure 8a - Model Average Heave Versus Model Velocity

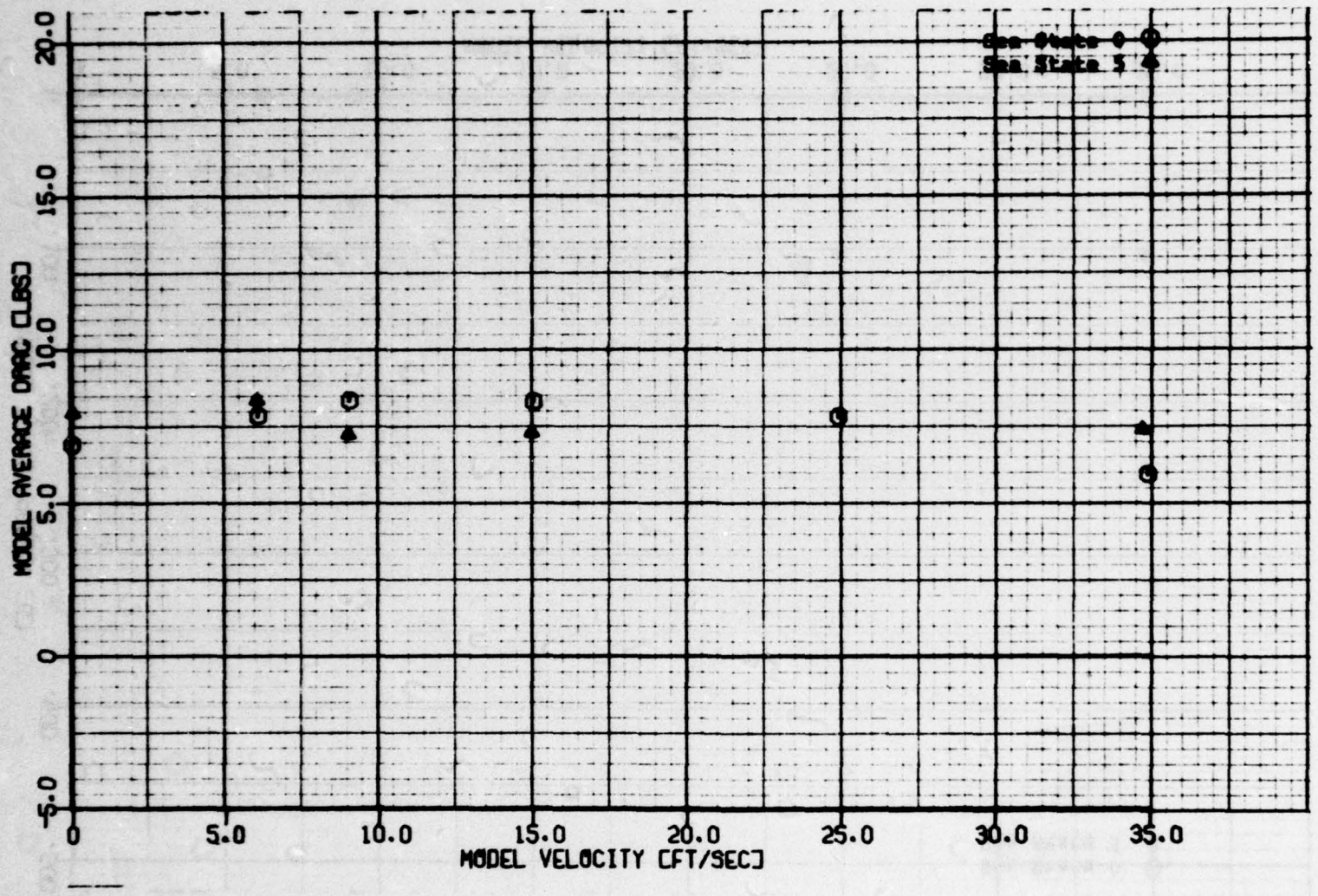

Figure 8b - Model Average Drag Versus Model Velocity

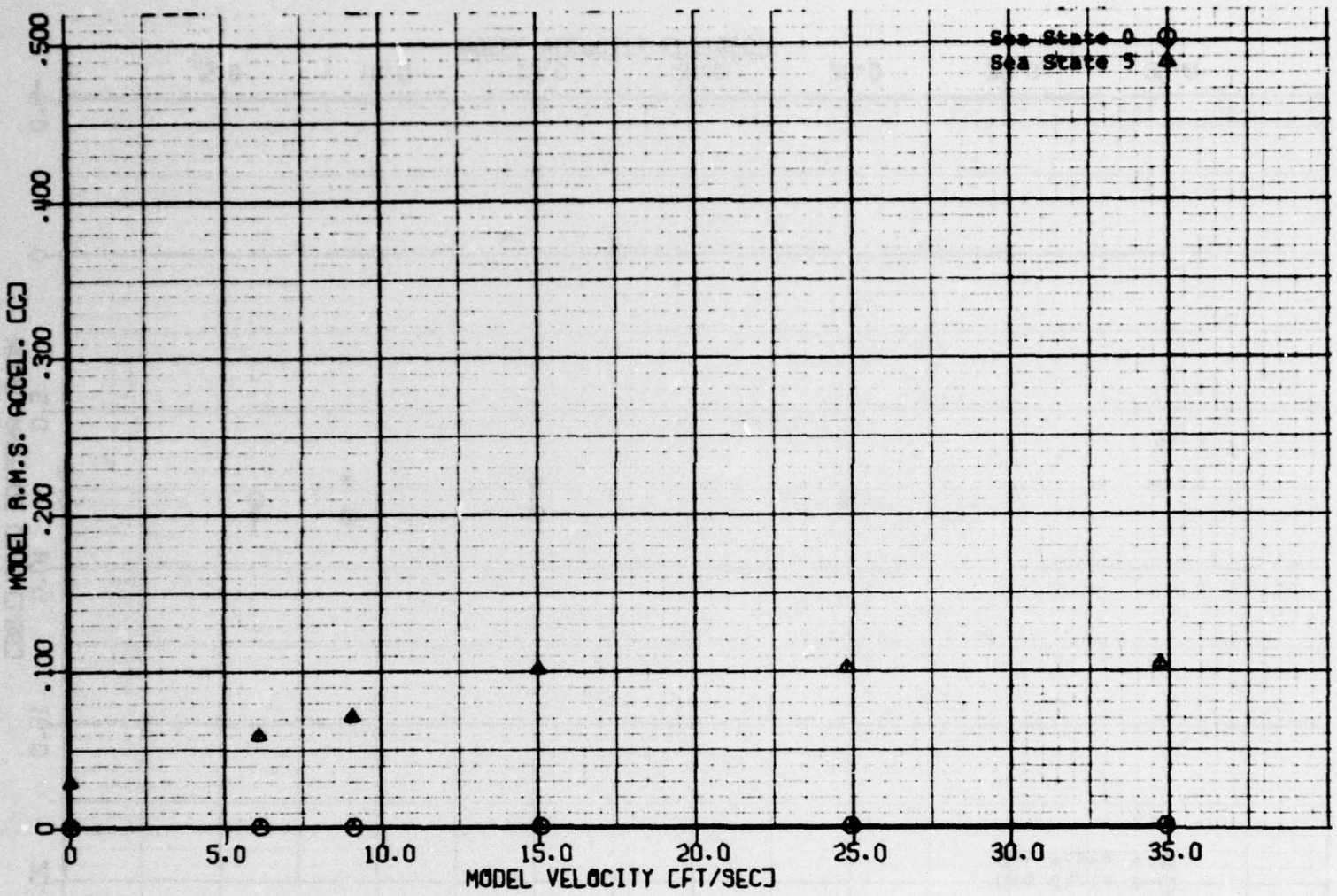

Figure 8c - Model RMS Acceleration Versus Model Velocity

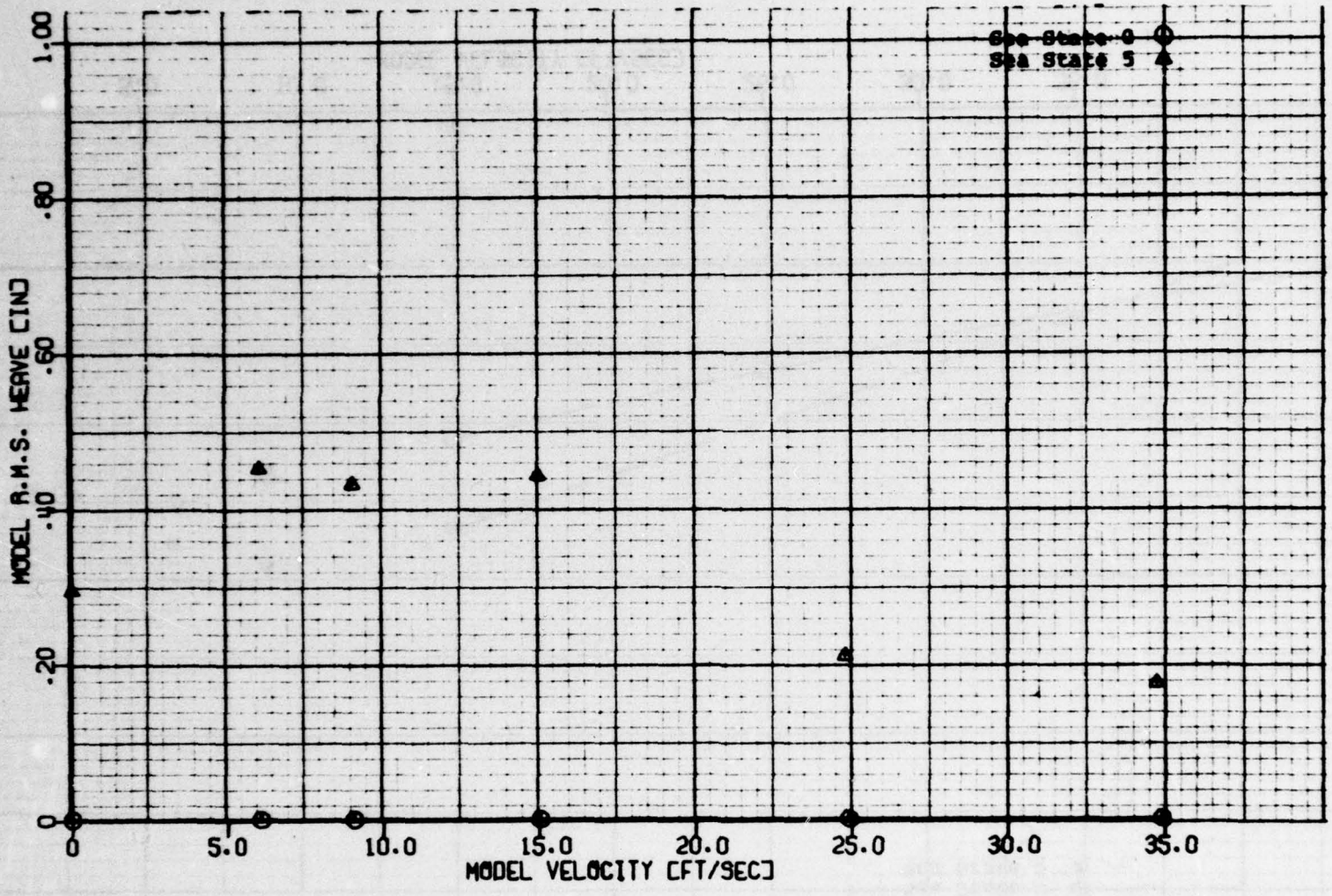

Figure 8d - Model RMS Heave Versus Model Velocity

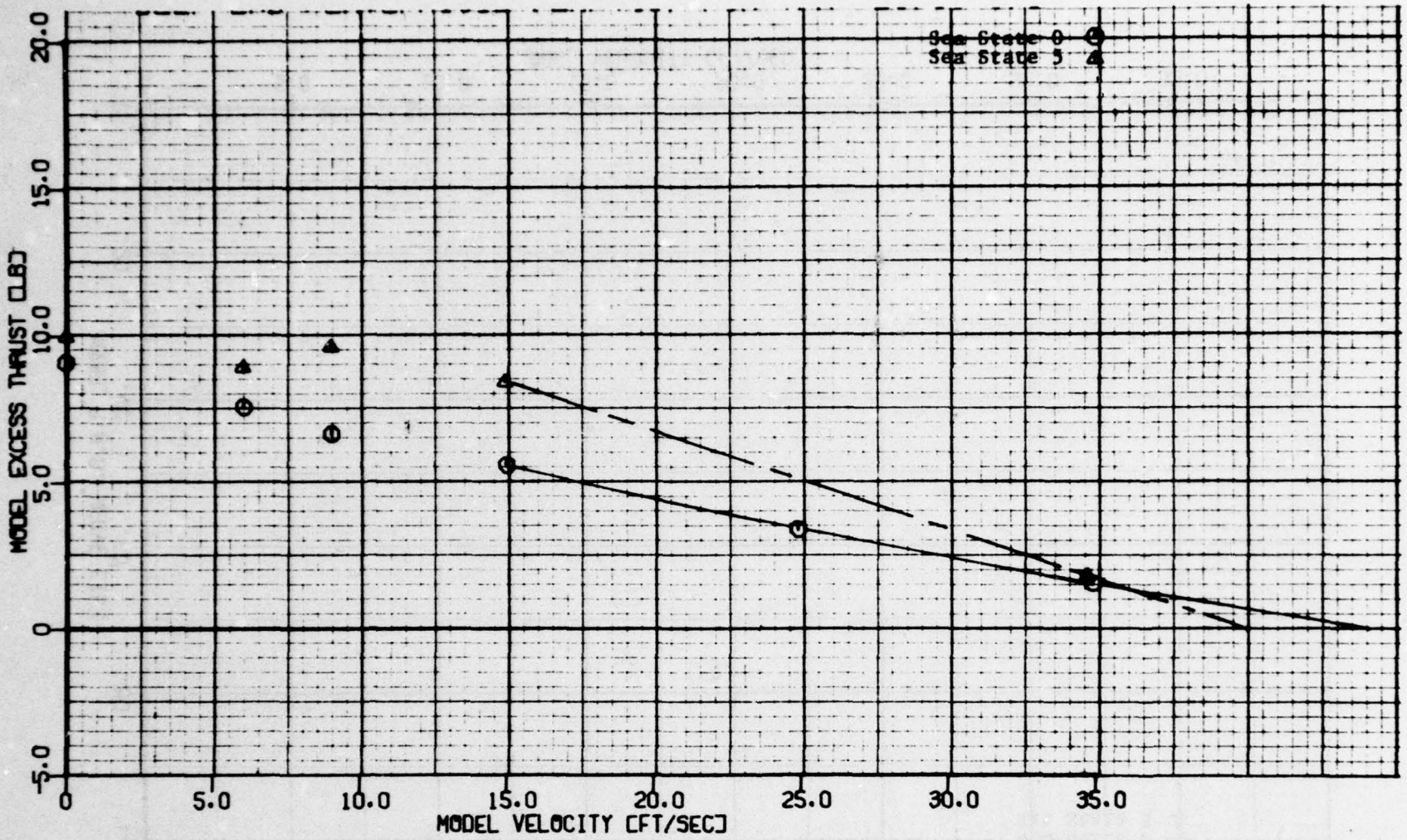

Figure 8e - Model Excess Thrust Versus Model Velocity

Figure 9 - Metal Endplate with Rigid Flap for T/W = 0.25 at Sea State 5

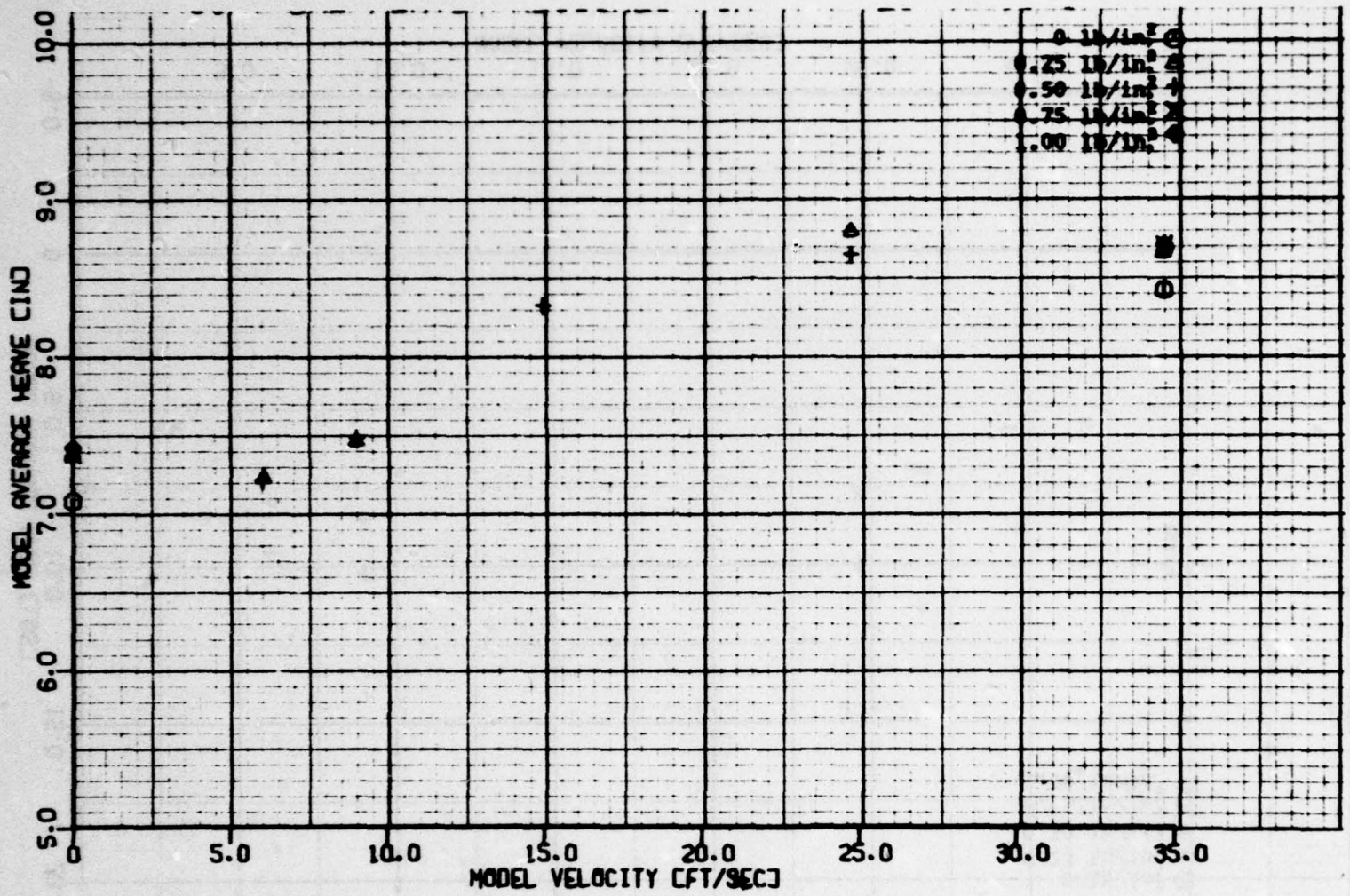

Figure 9a - Model Average Heave Versus Model Velocity

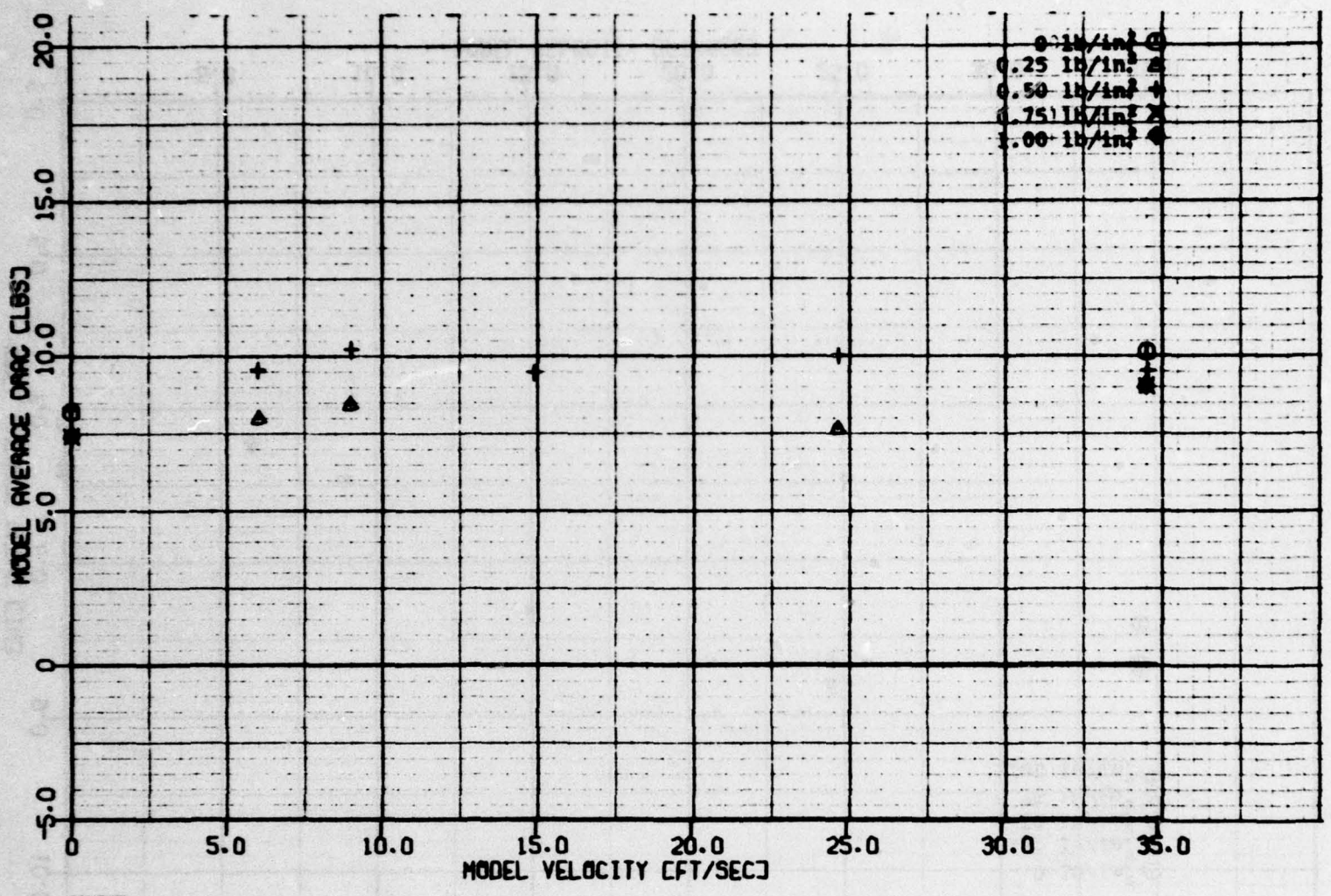

Figure 9b - Model Average Drag Versus Model Velocity

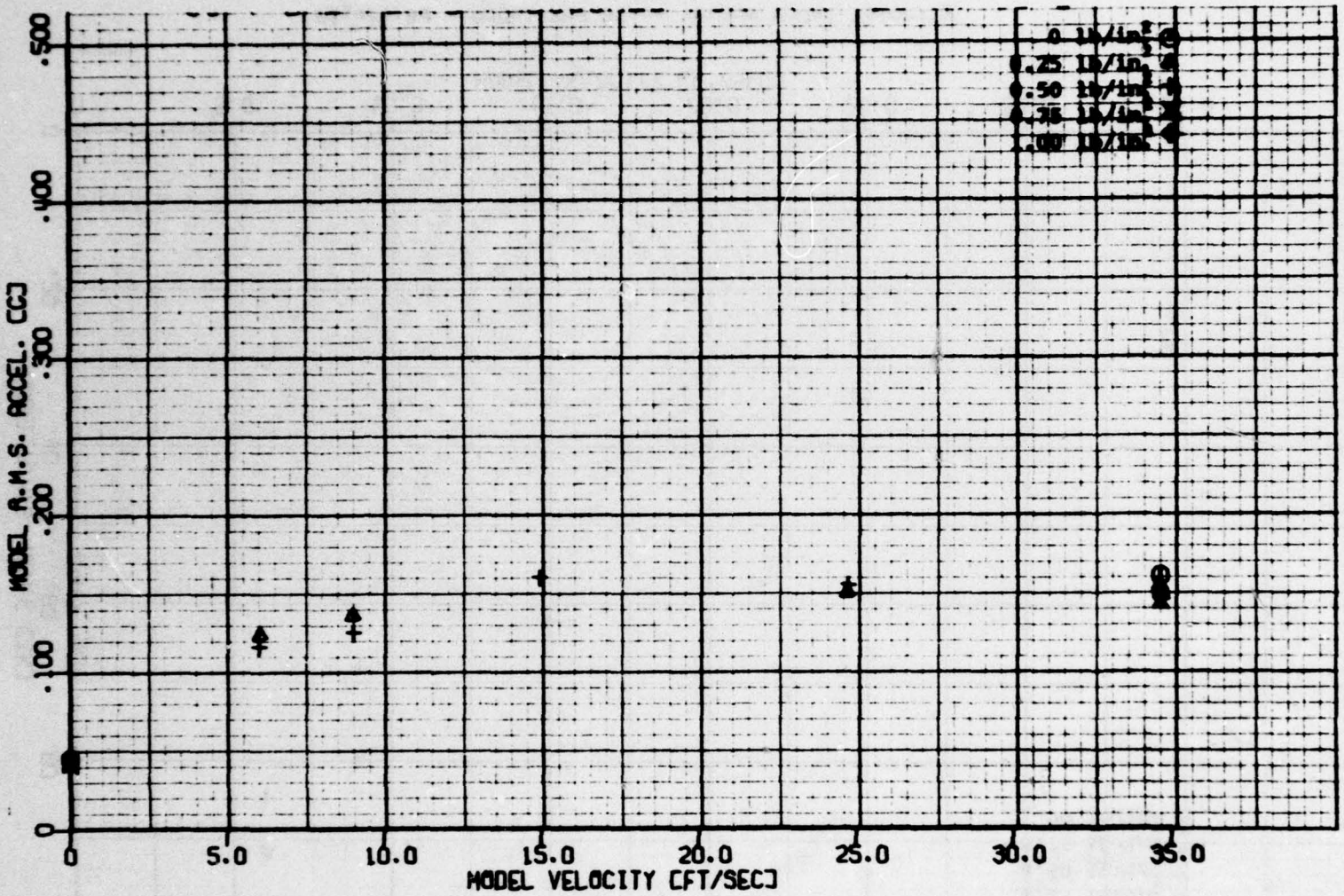

Figure 9c - Model RMS Acceleration Versus Model Velocity

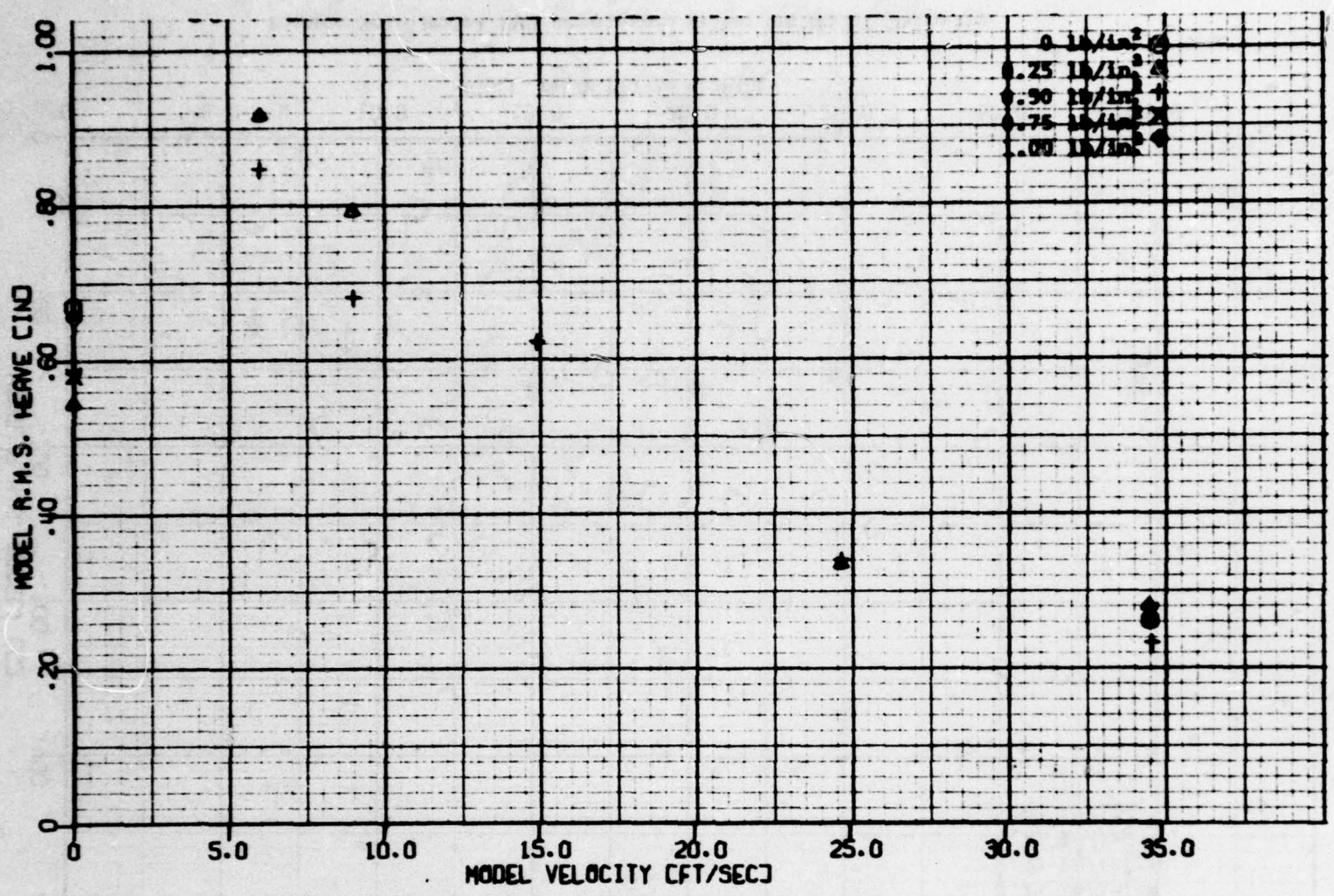

Figure 9d - Model RMS Heave Versus Model Velocity

Figure 10 - Soft Endplate for T/W = 0.25 at Sea States 0, 4, and 5

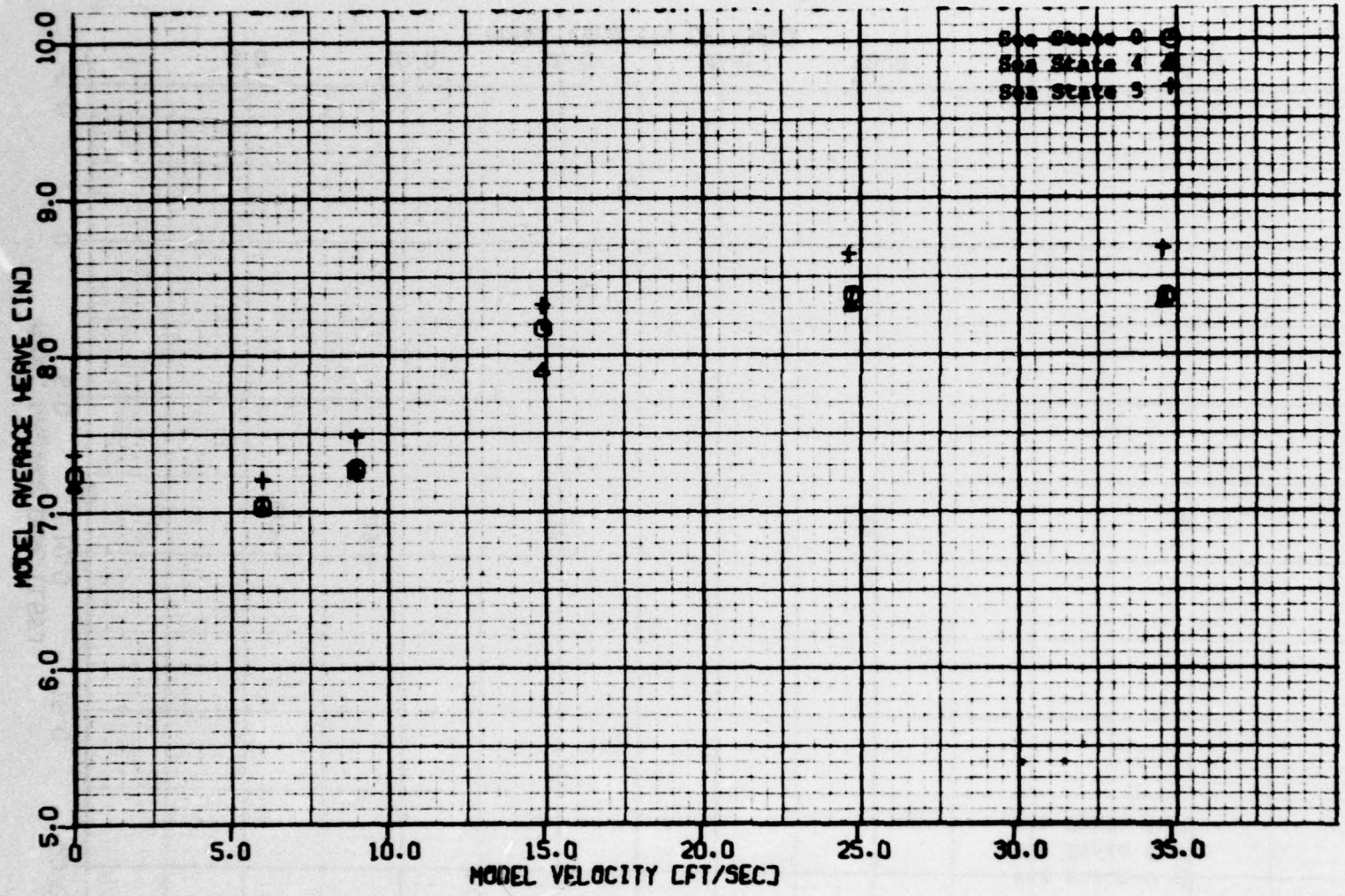

Figure 10a - Model Average Heave Versus Model Velocity

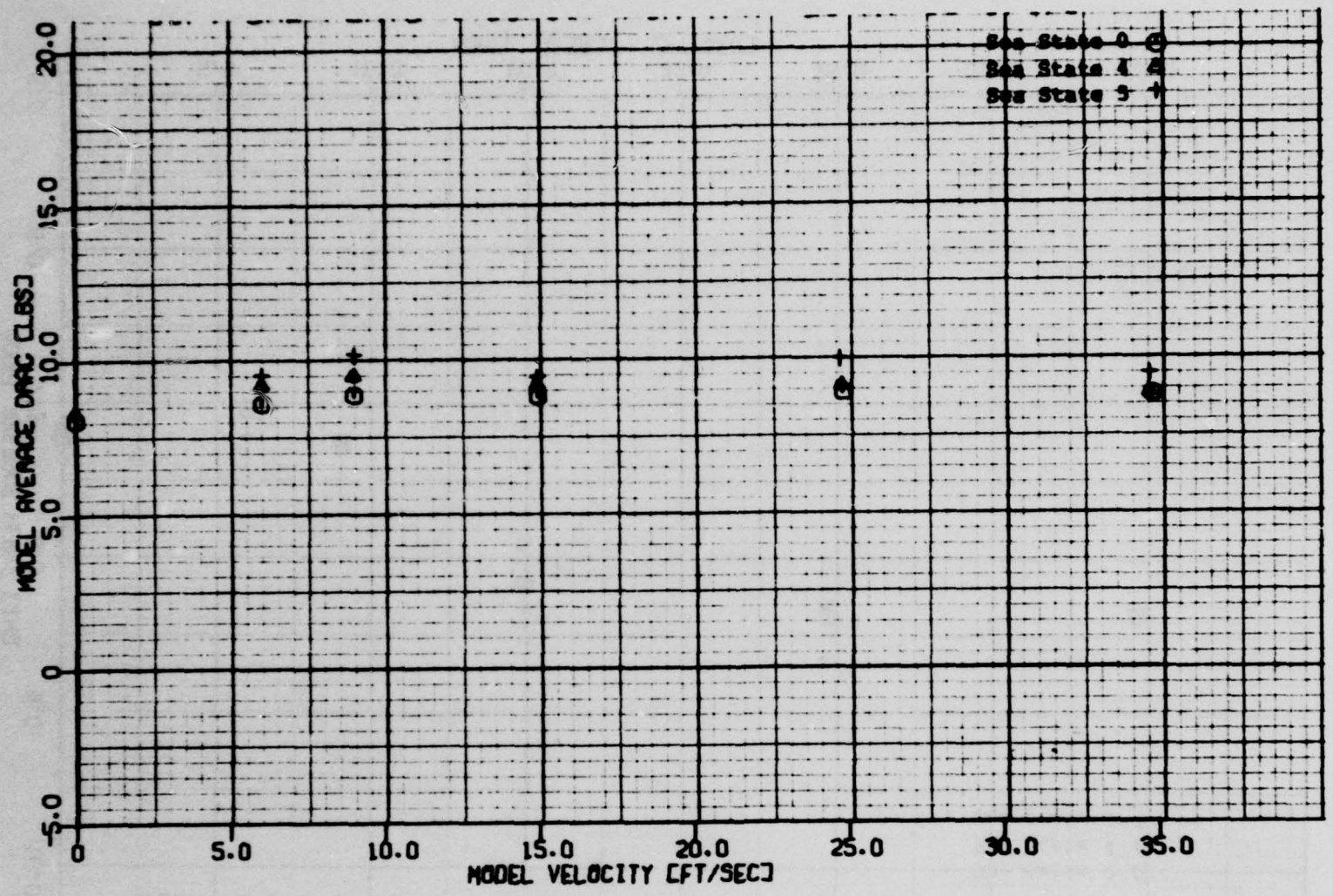

Figure 10b - Model Average Drag Versus Model Velocity

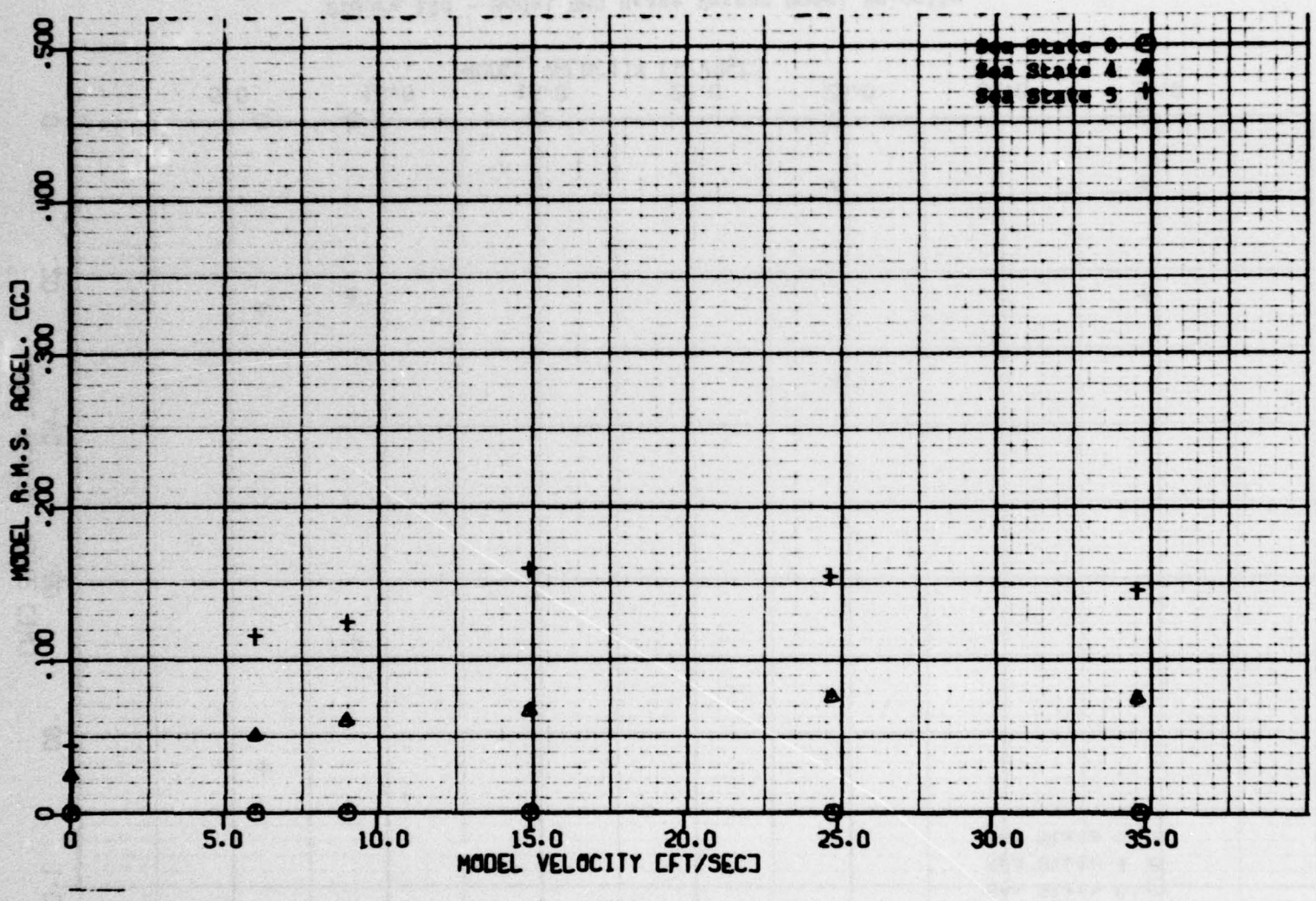

Figure 10c - Model RMS Acceleration Versus Model Velocity

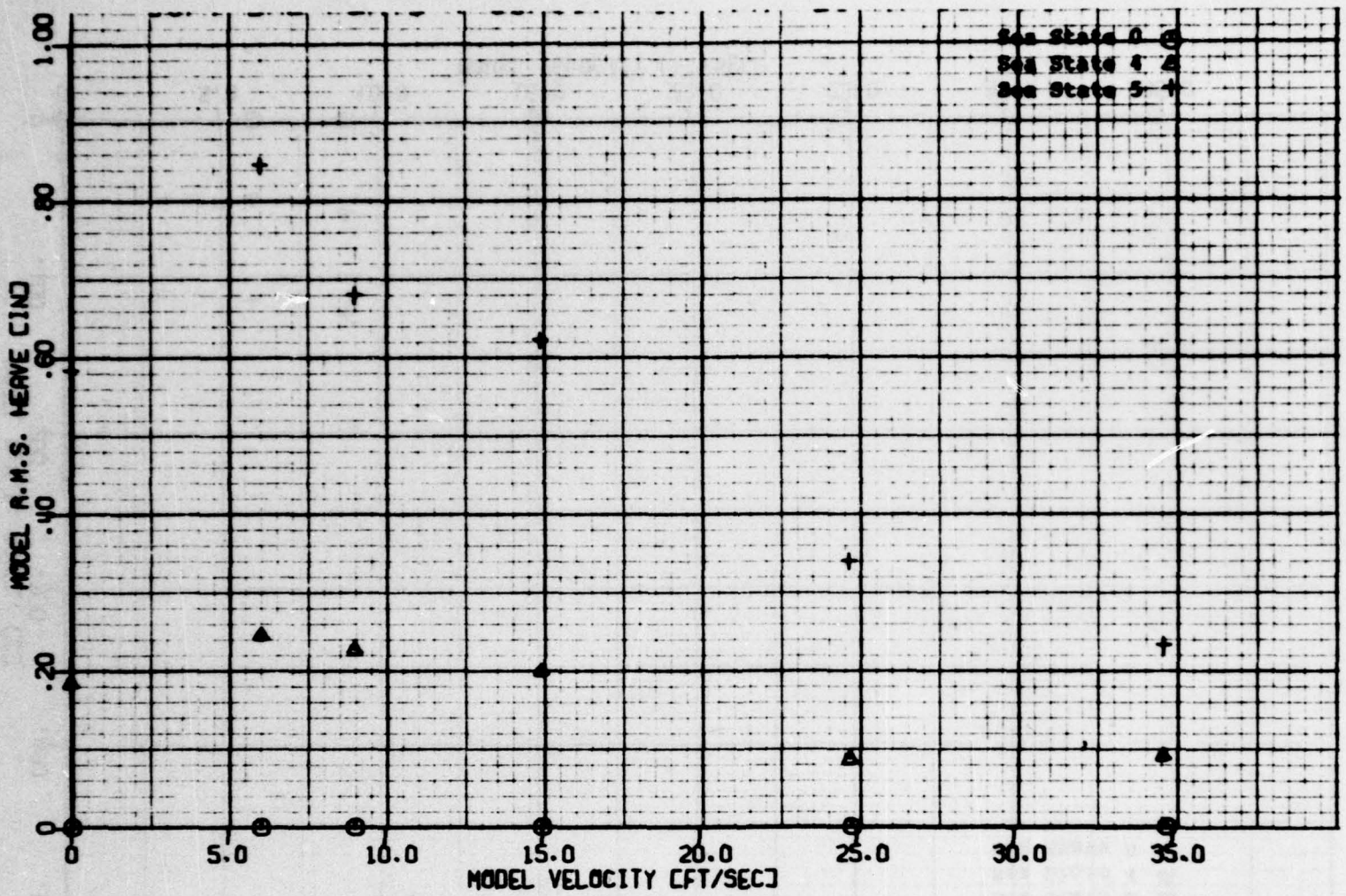

Figure 10d - Model RMS Heave Versus Model Velocity

Figure 11 - Soft Endplate for T/W = 0.20 Versus T/W = 0.25 at Sea State 5

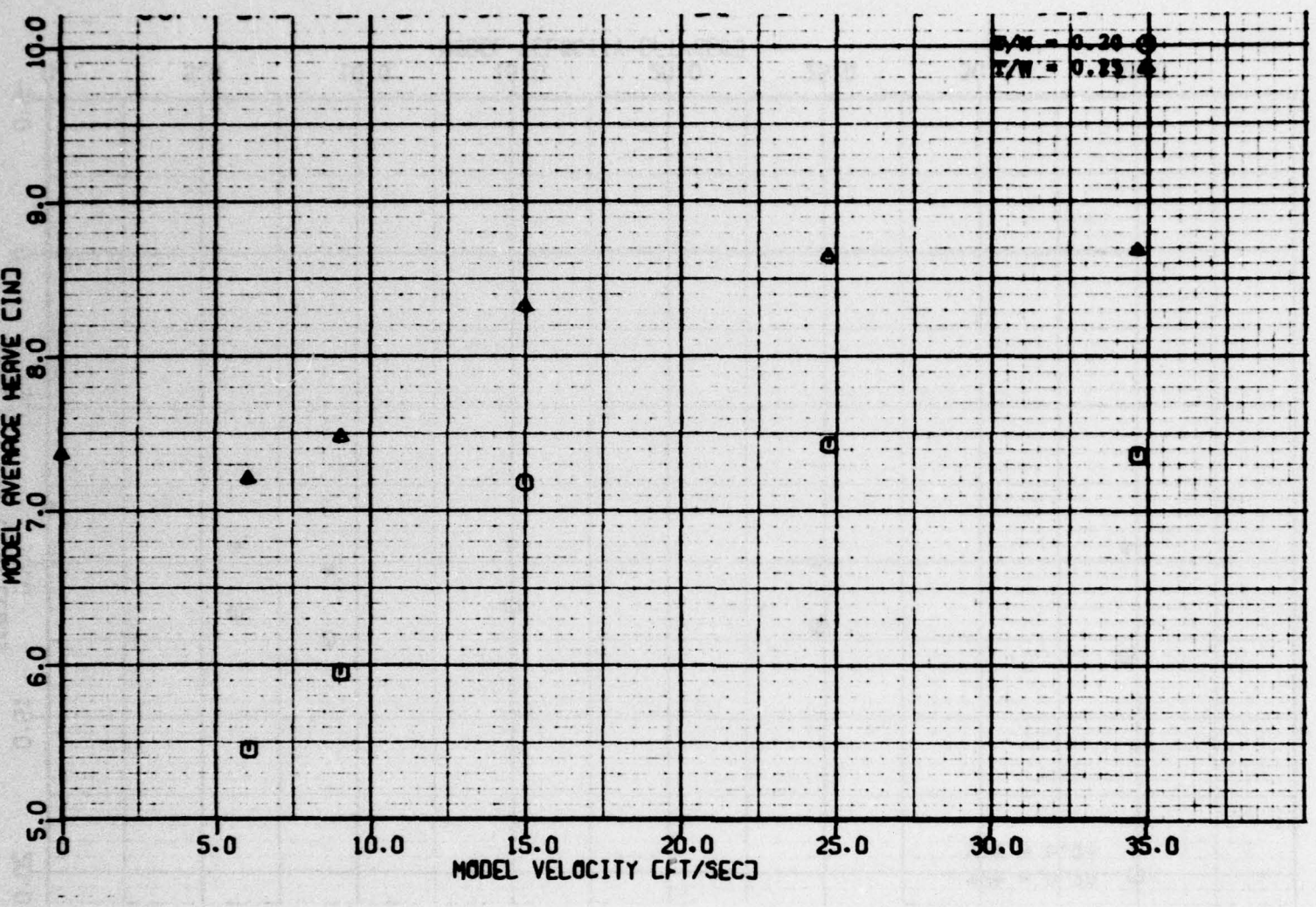

Figure 11a - Model Average Heave Versus Model Velocity

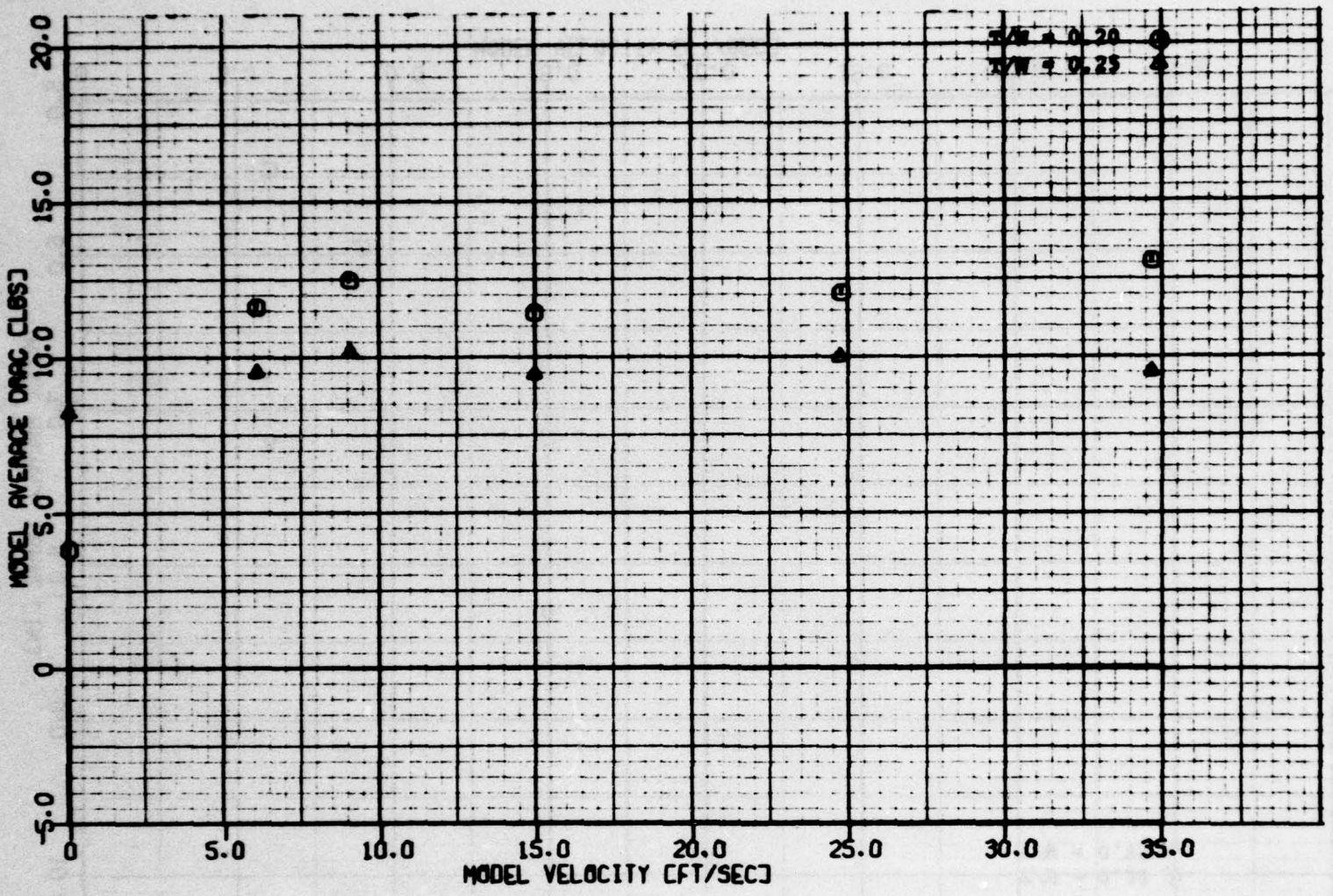

Figure 11b - Model Average Drag Versus Model Velocity

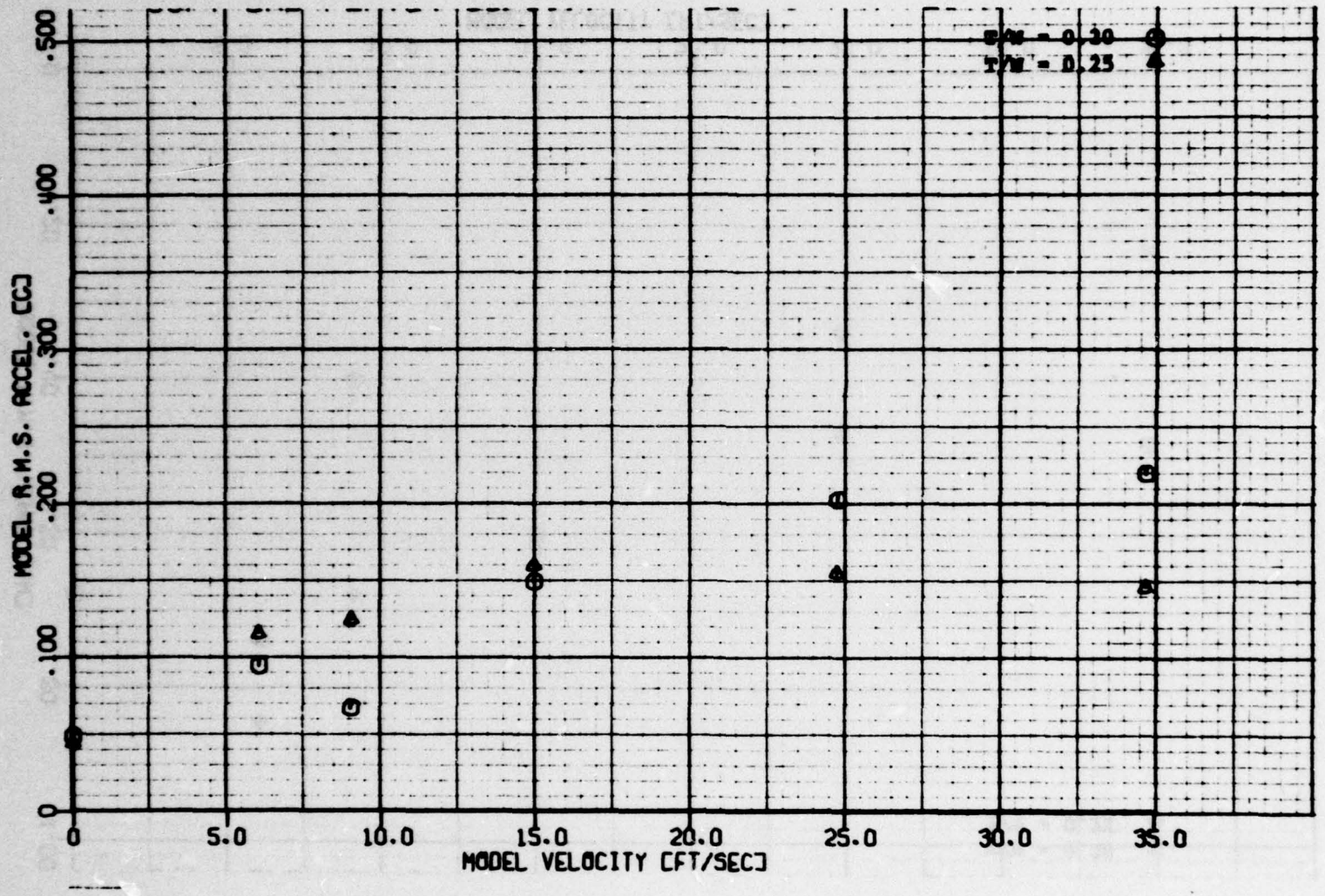

Figure 11c - Model RMS Acceleration Versus Model Velocity

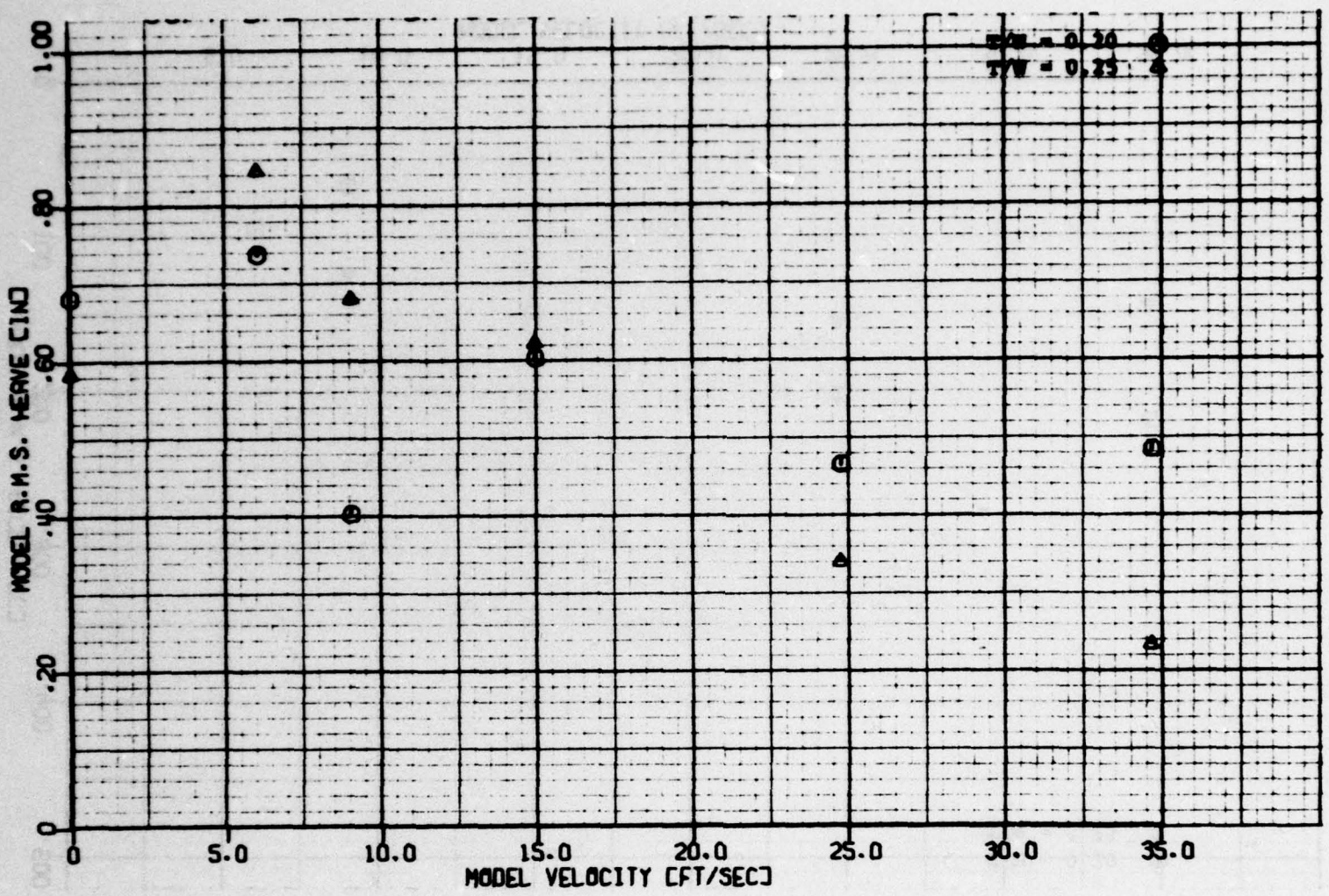

Figure 11d - Model RMS Heave Versus Model Velocity

Figure 12 - Basic Rigid Versus Soft Endplate for T/W = 0.25 at Sea State 5

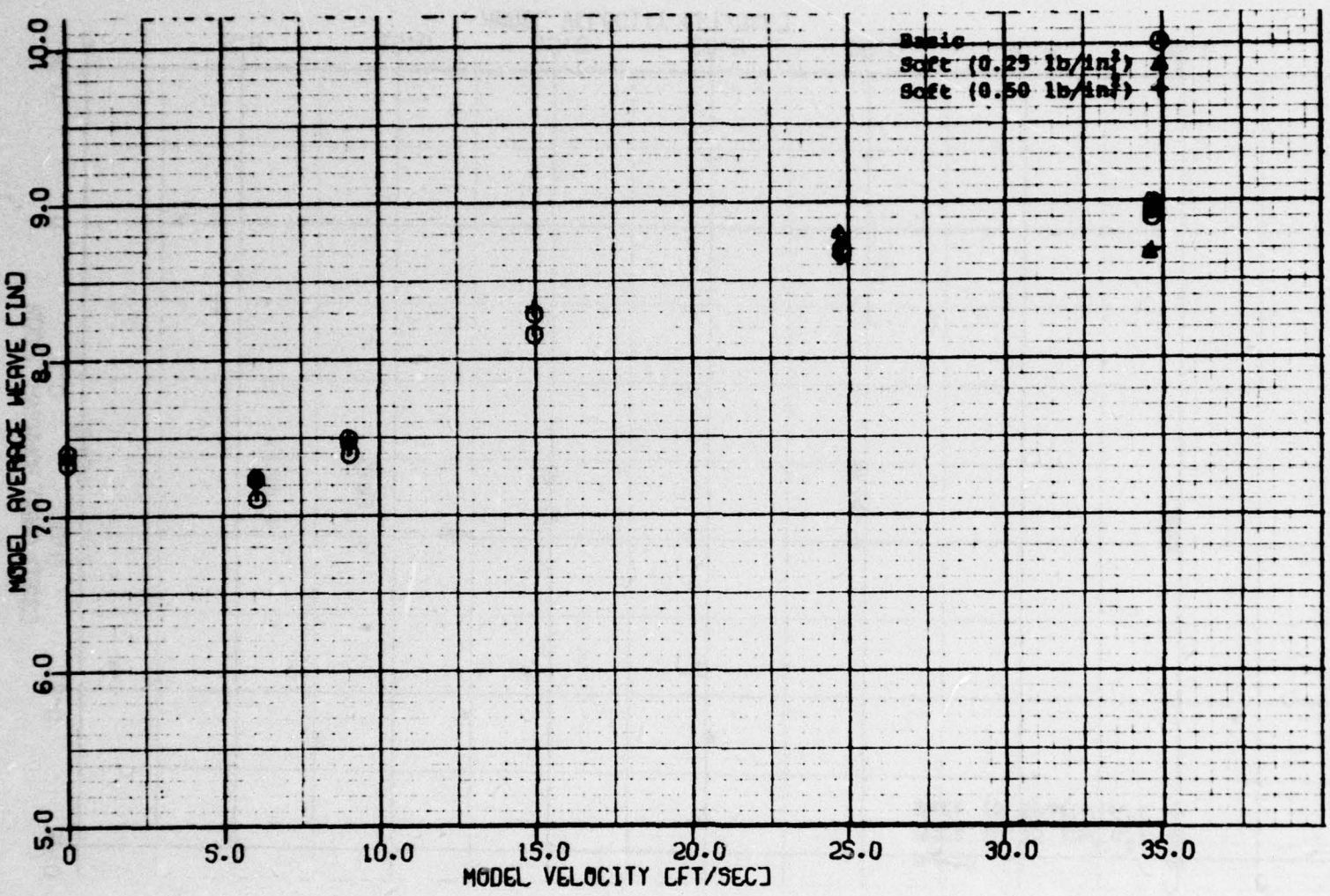

Figure 12a - Model Average Heave Versus Model Velocity

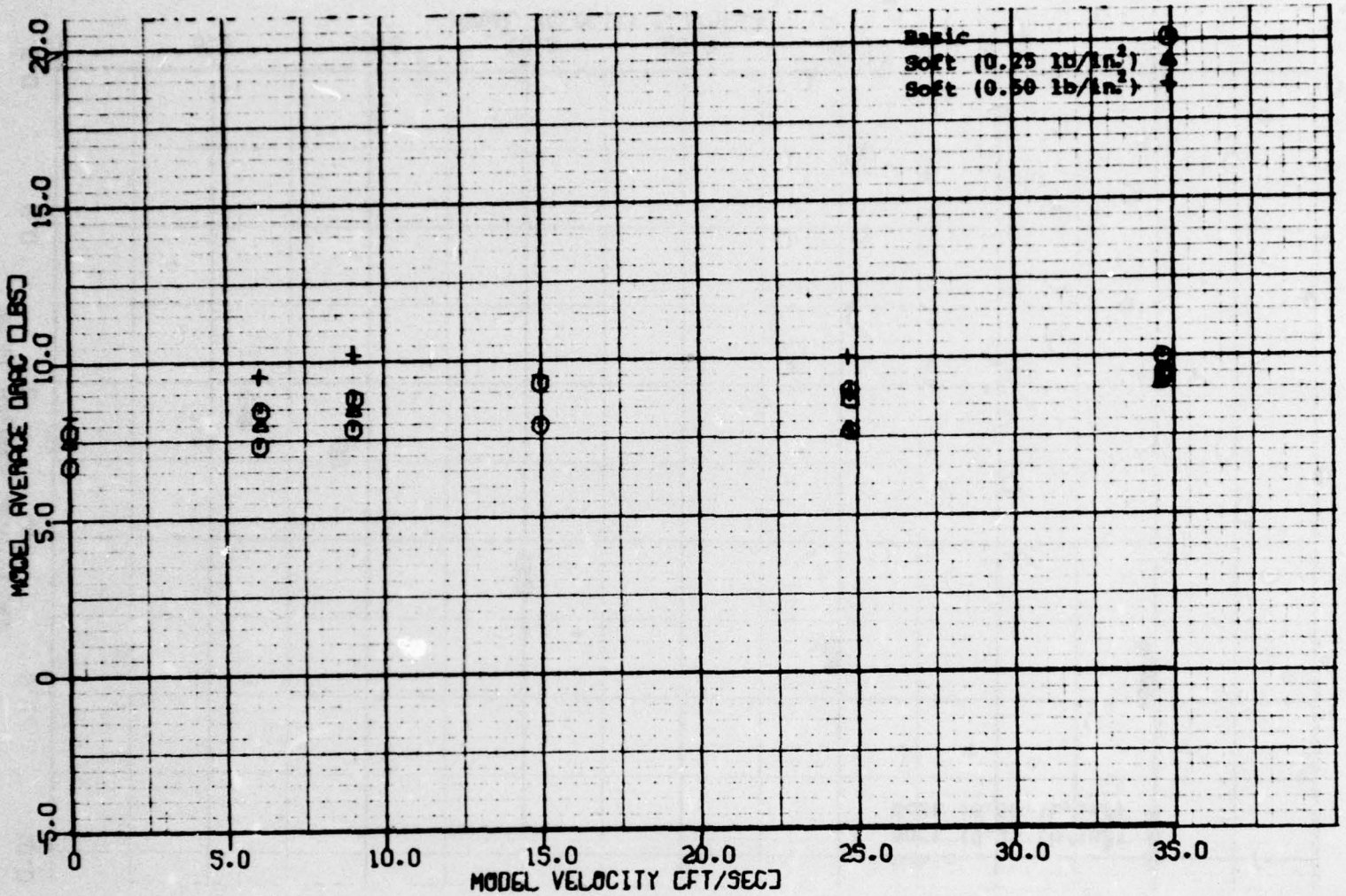

Figure 12b - Model Average Drag Versus Model Velocity

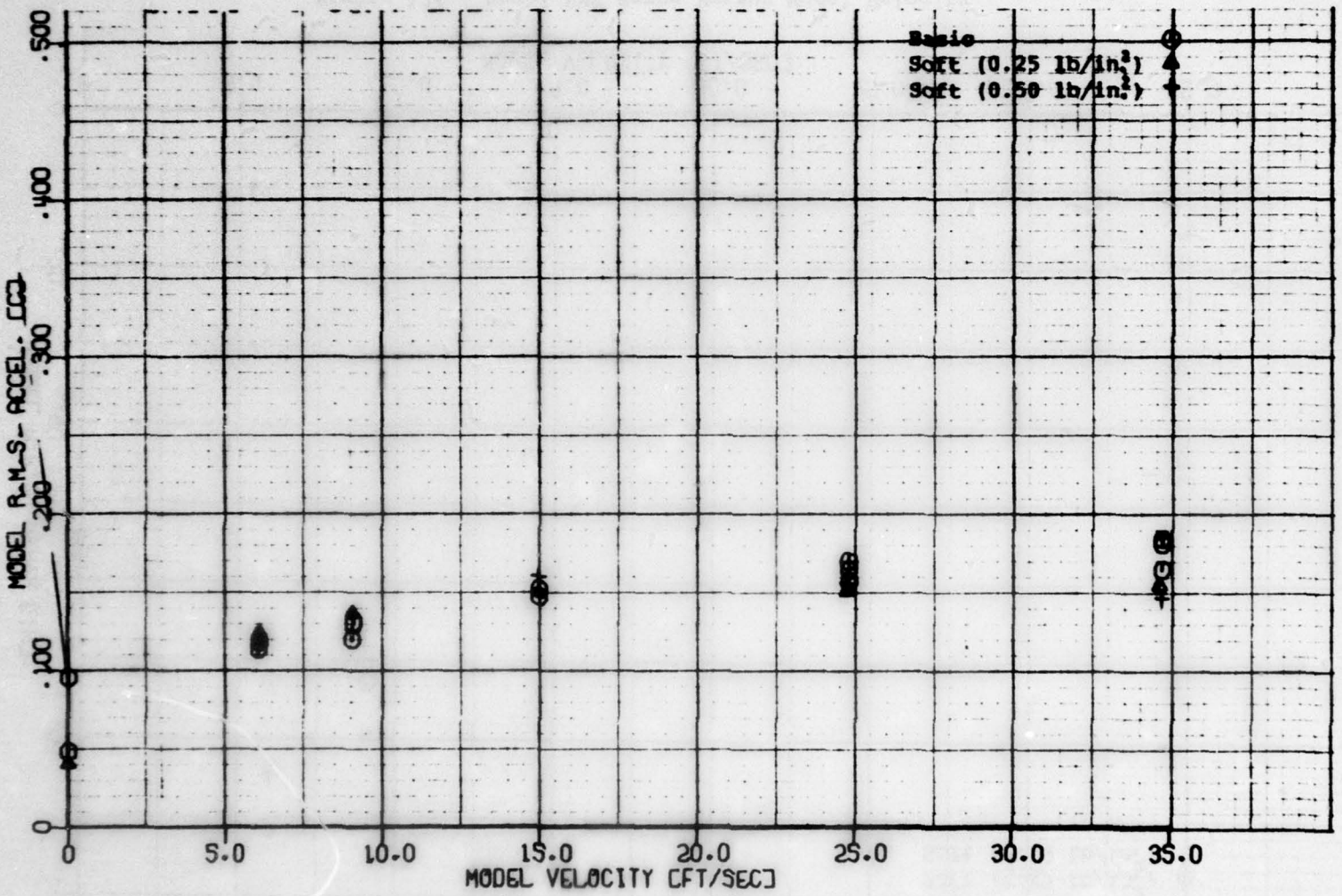

Figure 12c - Model RMS Acceleration Versus Model Velocity

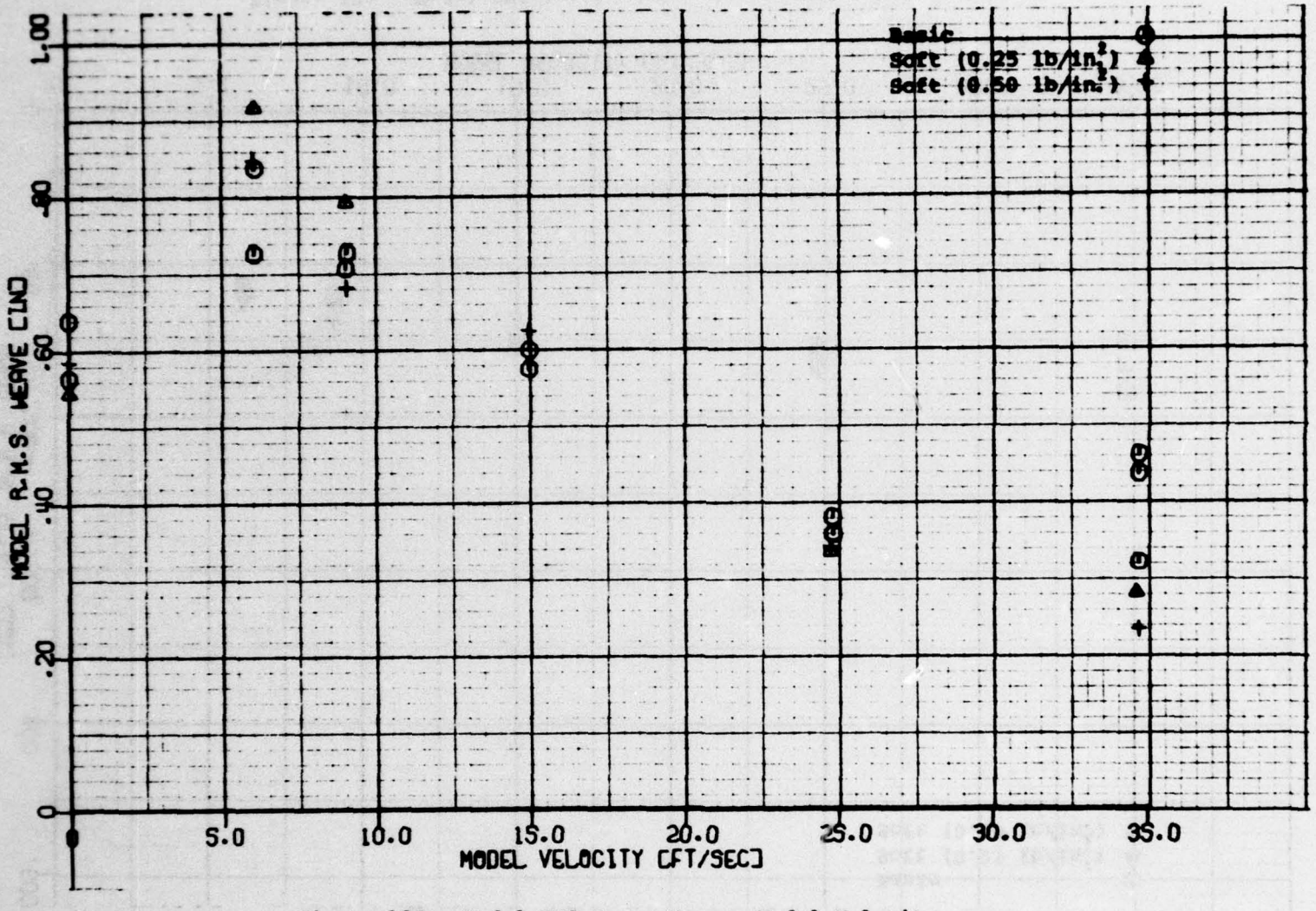

Figure 12d - Model RMS Heave Versus Model Velocity

Figure 13 - Two-Spring Bumper with Various Stiffnesses for T/W = 0.25 at Sea State 5

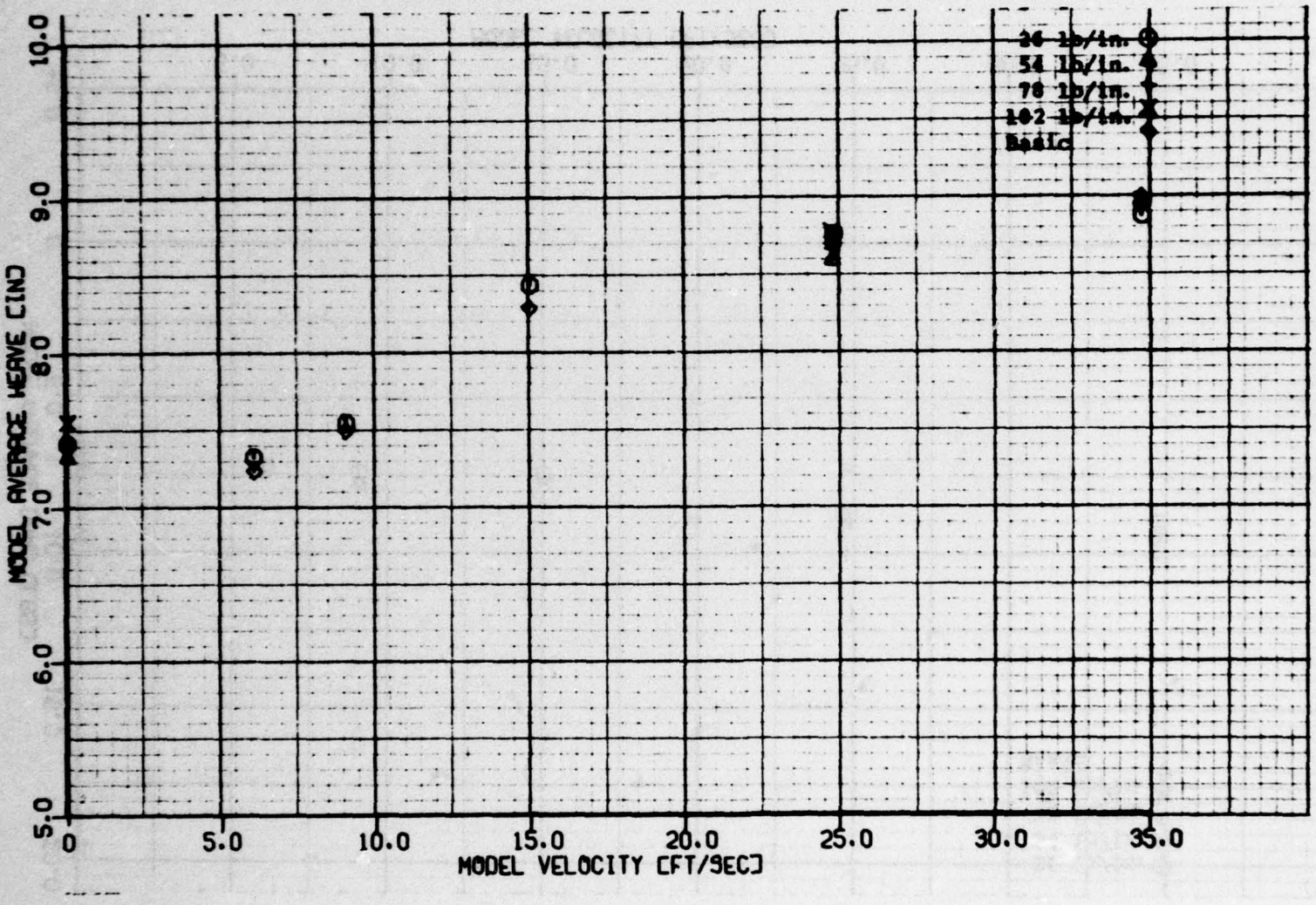

Figure 13a - Model Average Heave Versus Model Velocity

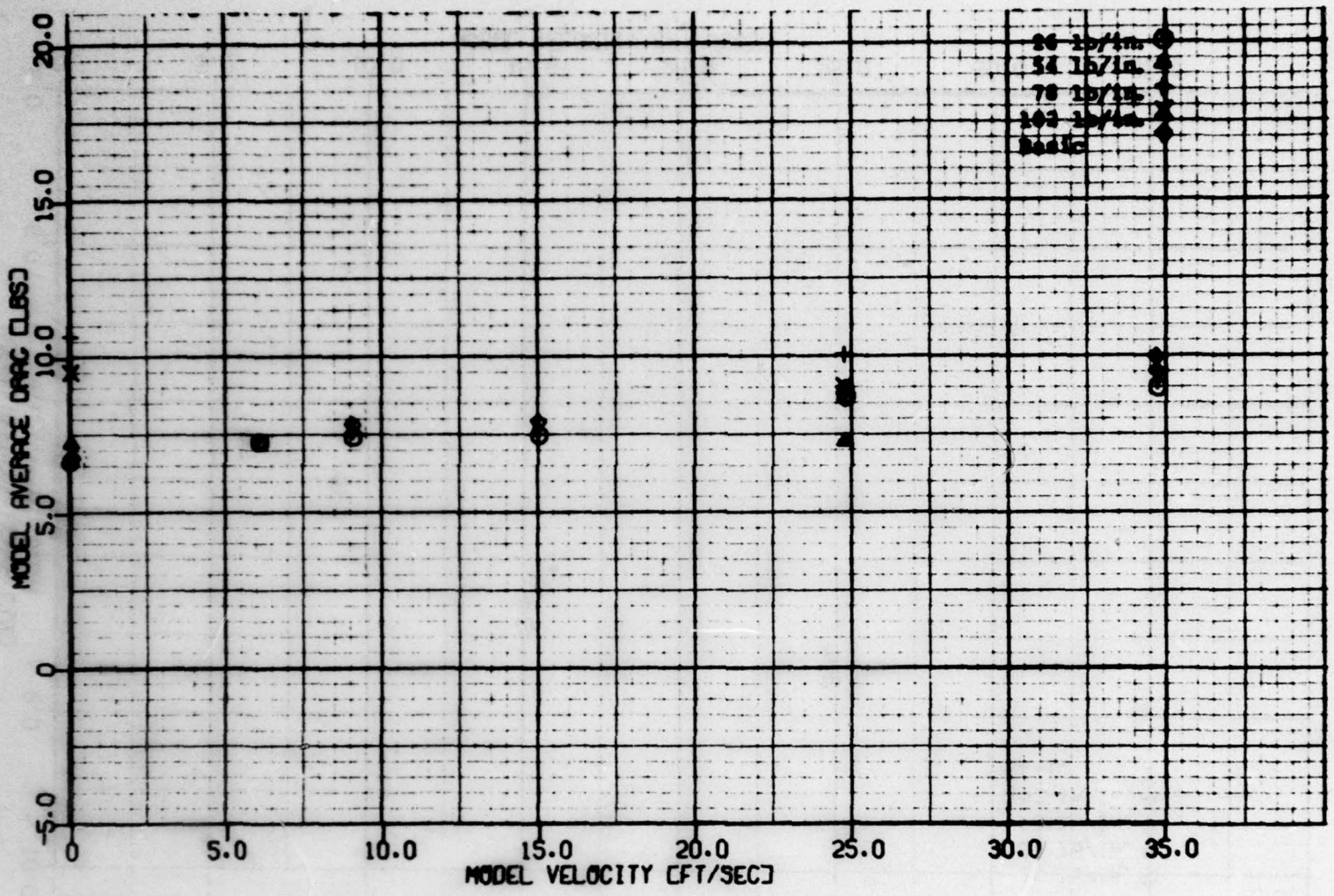

Figure 13b - Model Average Drag Versus Model Velocity

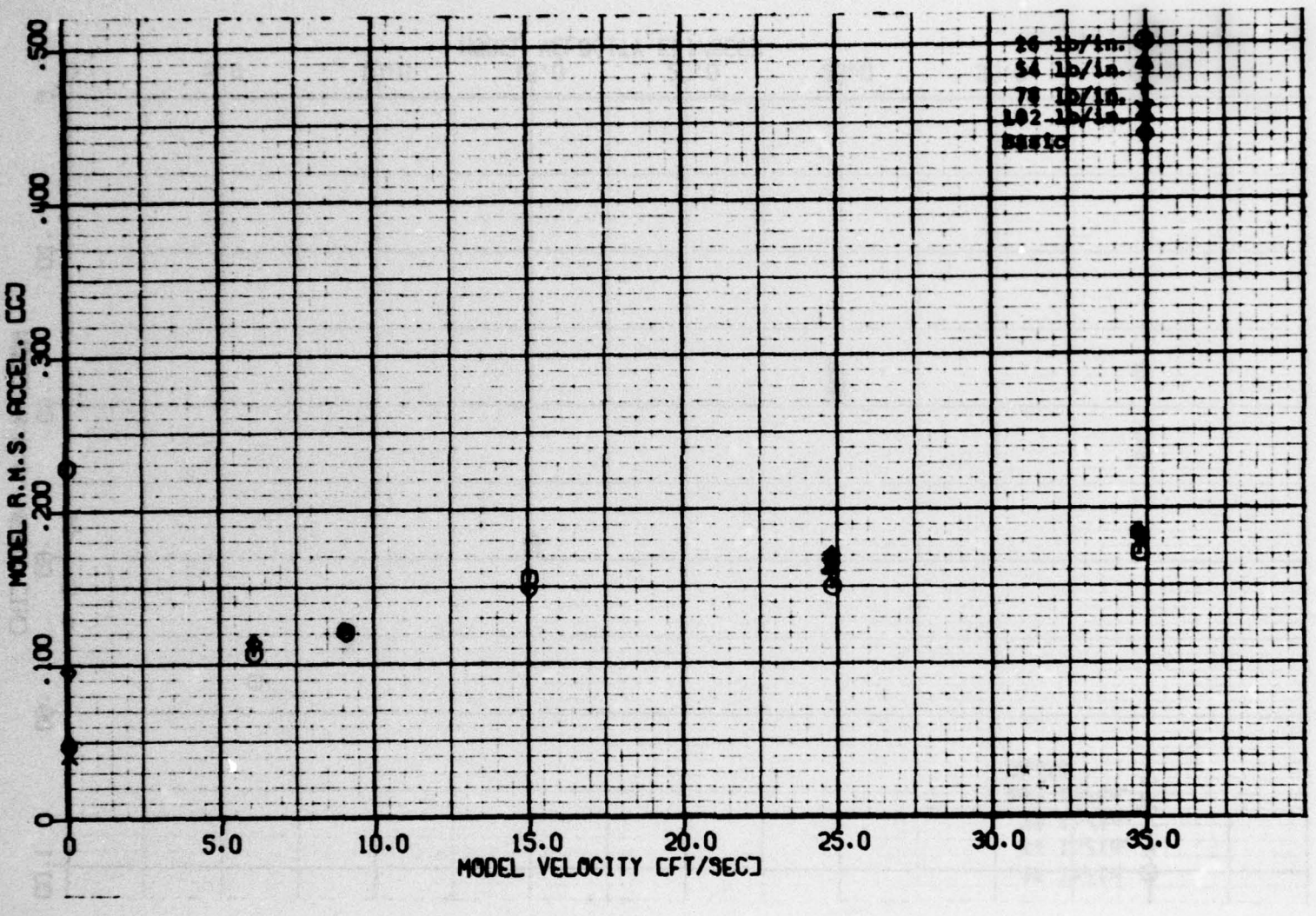

Figure 13c - Model RMS Acceleration Versus Model Velocity

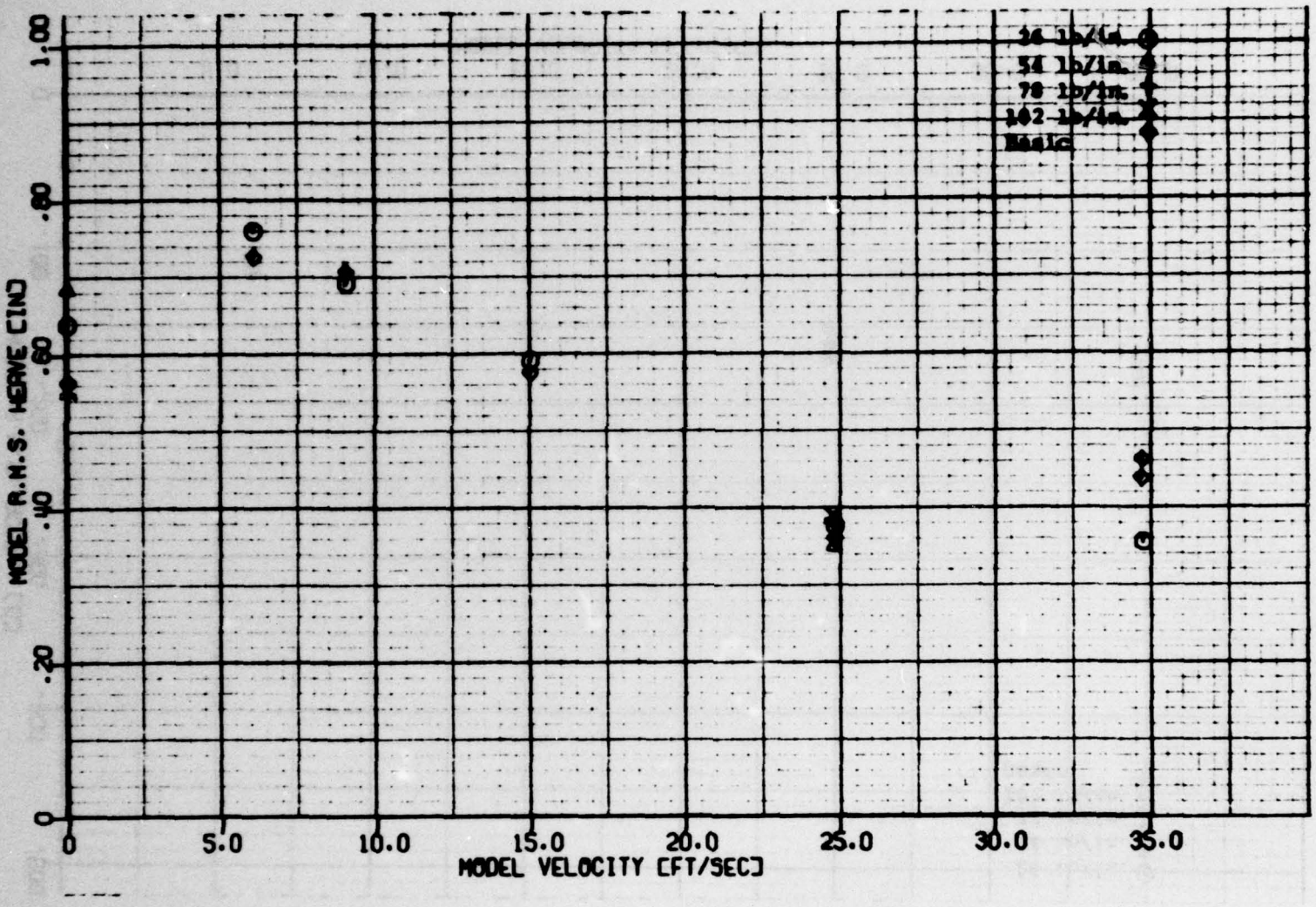

Figure 13d - Model RMS Heave Versus Model Velocity

Figure 14 - Basic Rigid Endplate for T/W = 0.25 at Sea States 0, 4, and 5

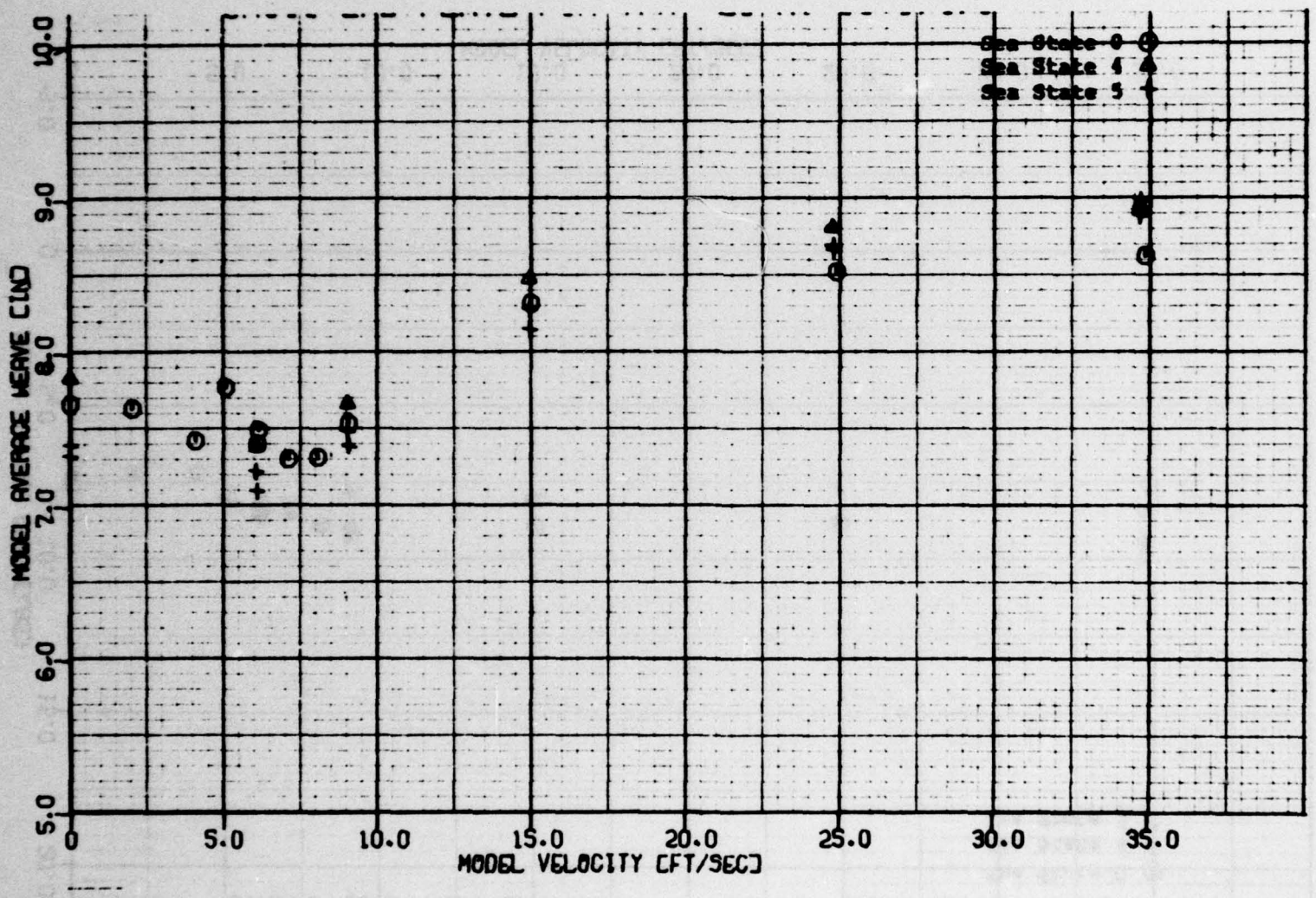

Figure 14a - Model Average Heave Versus Model Velocity

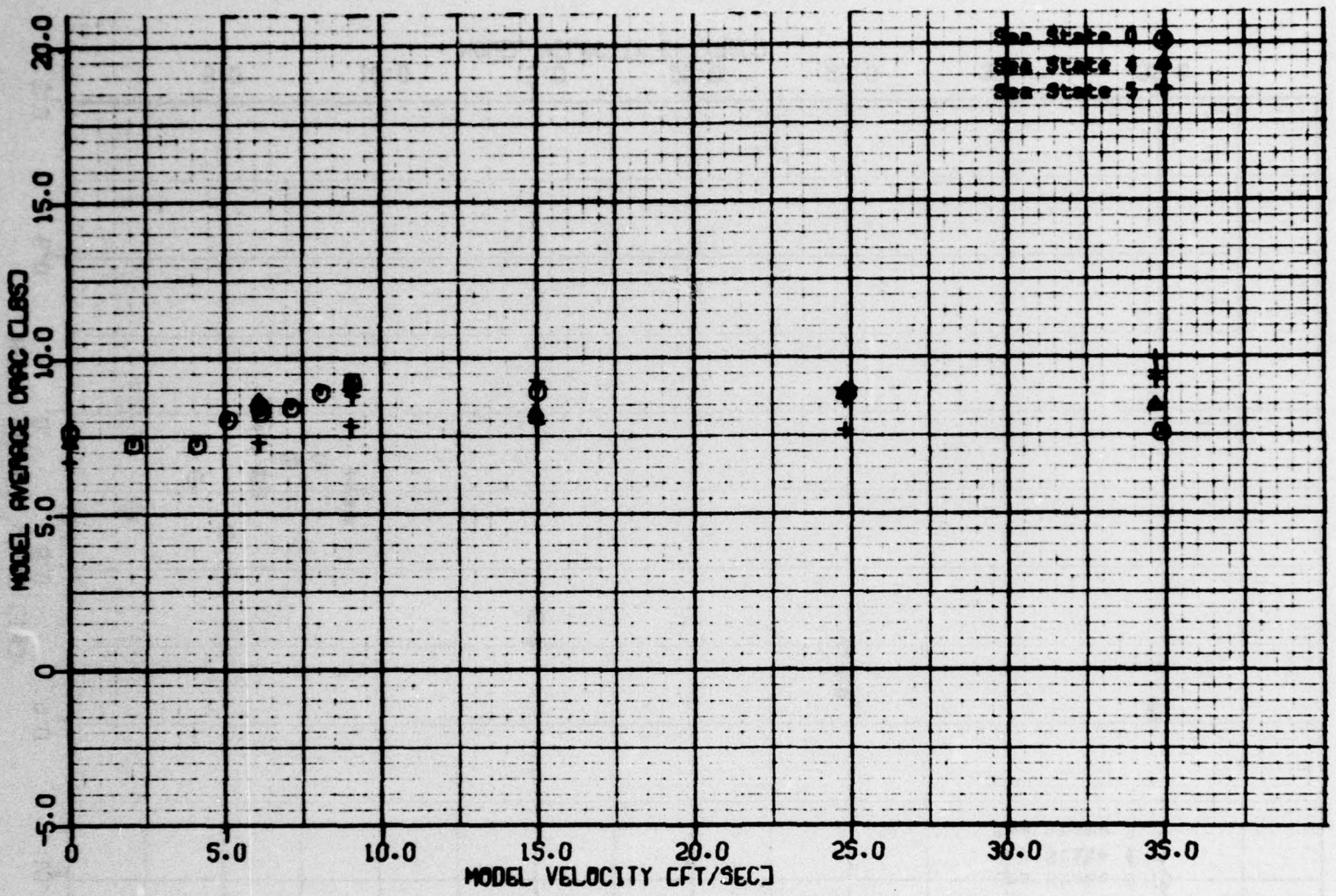

Figure 14b - Model Average Drag Versus Model Velocity

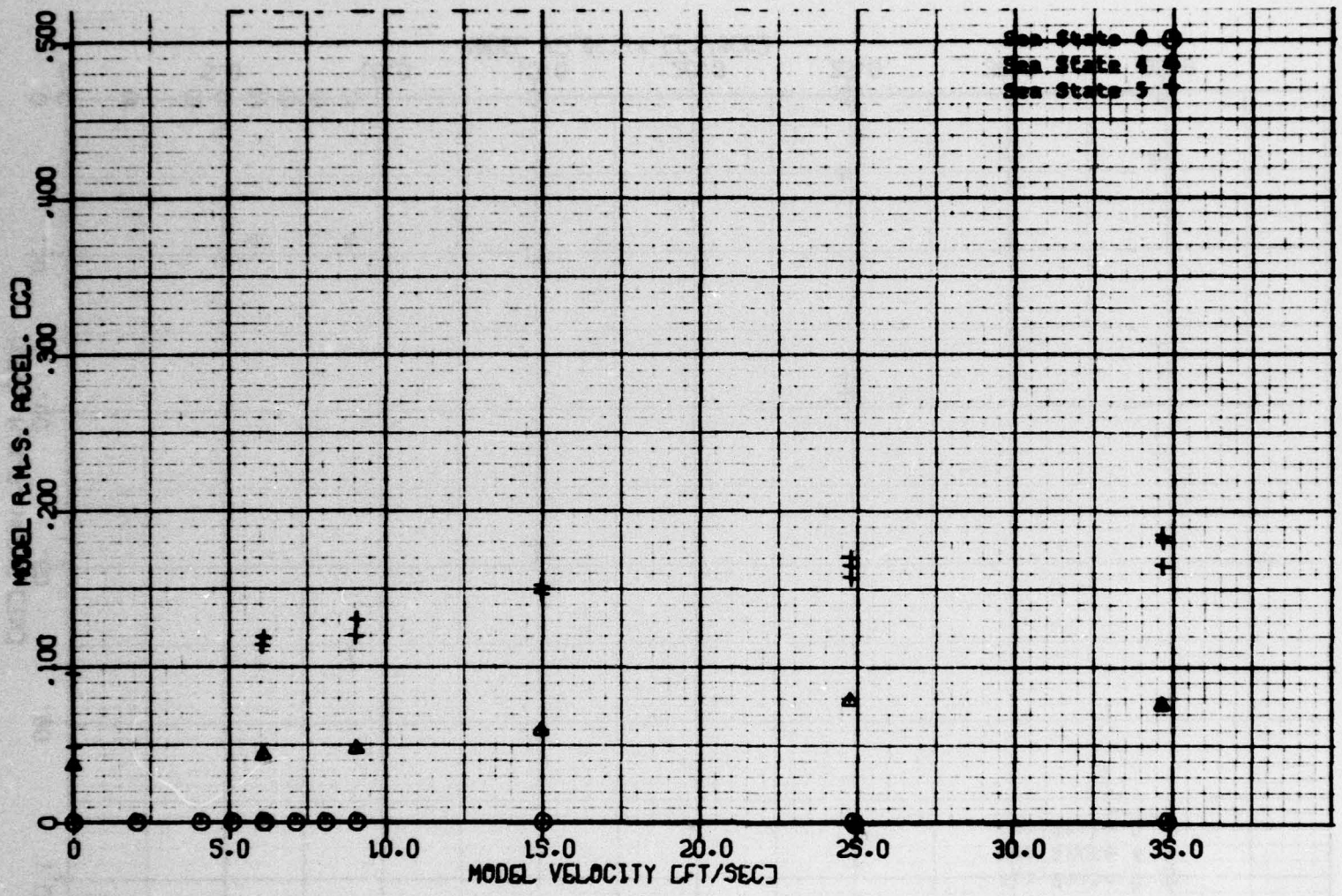

Figure 14c - Model RMS Acceleration Versus Model Velocity

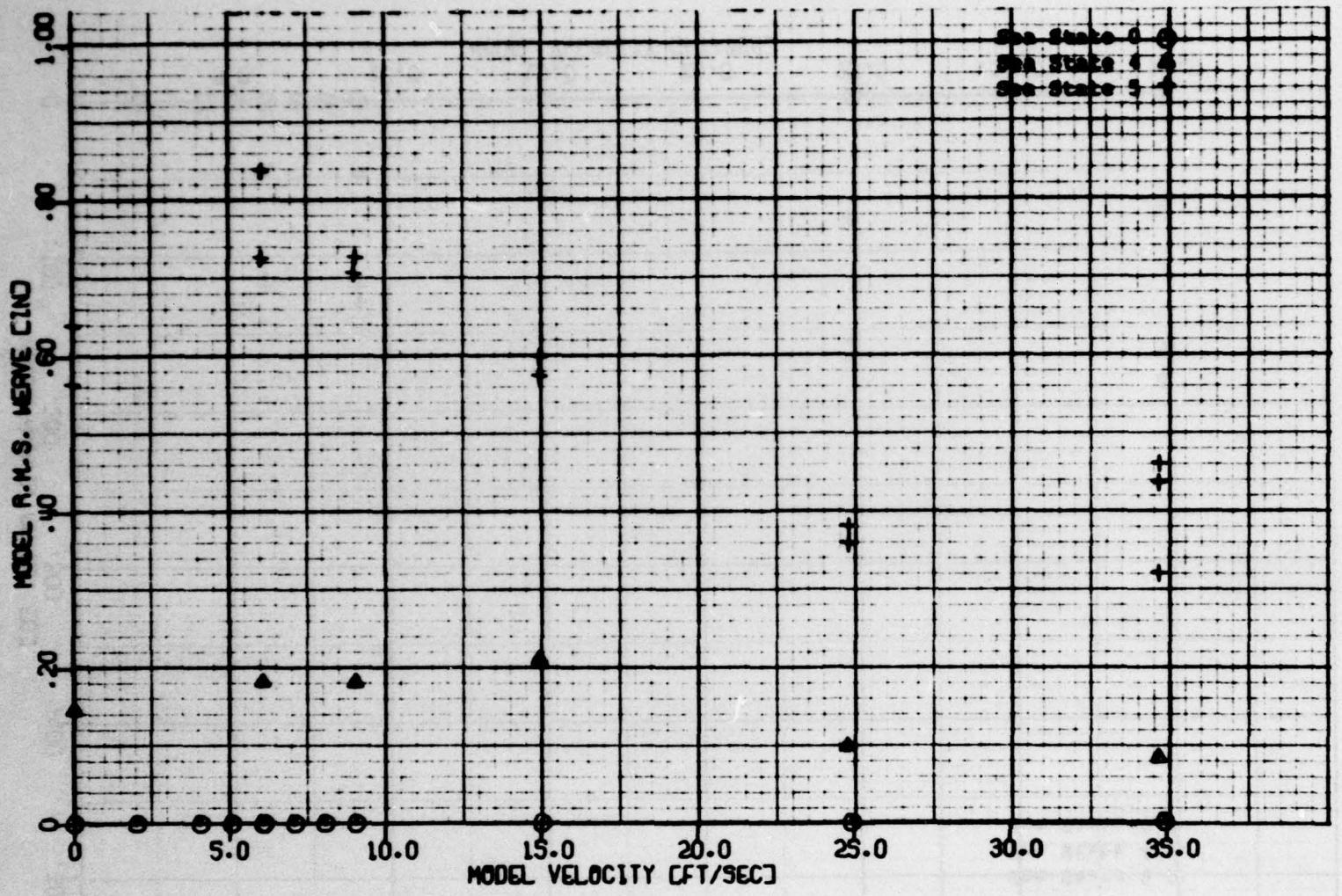

Figure 14d - Model RMS Heave Versus Model Velocity

Figure 15 - Basic Rigid Endplate for T/W = 0.20 Versus T/W = 0.25 at Sea State 0

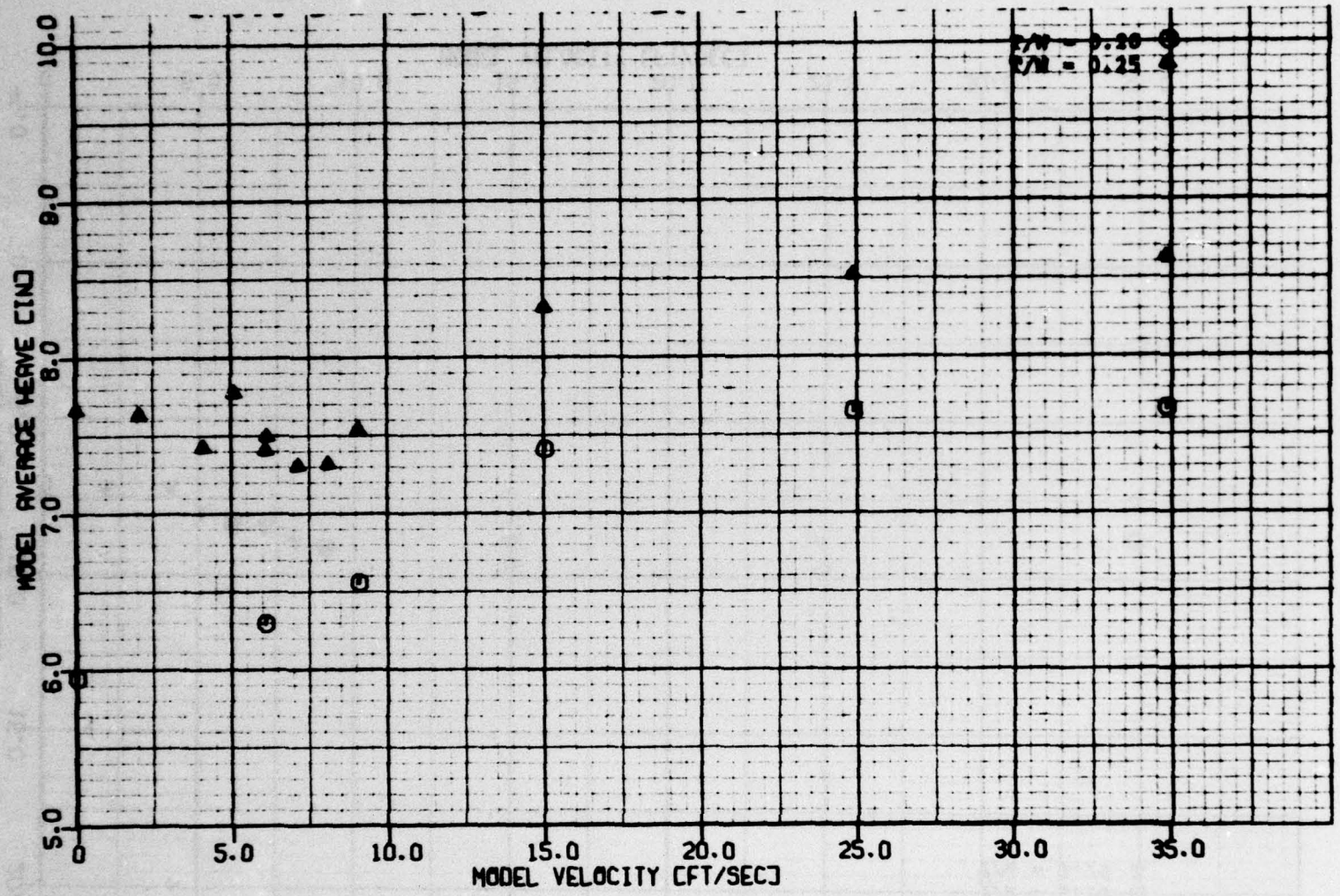

Figure 15a - Model Average Heave Versus Model Velocity

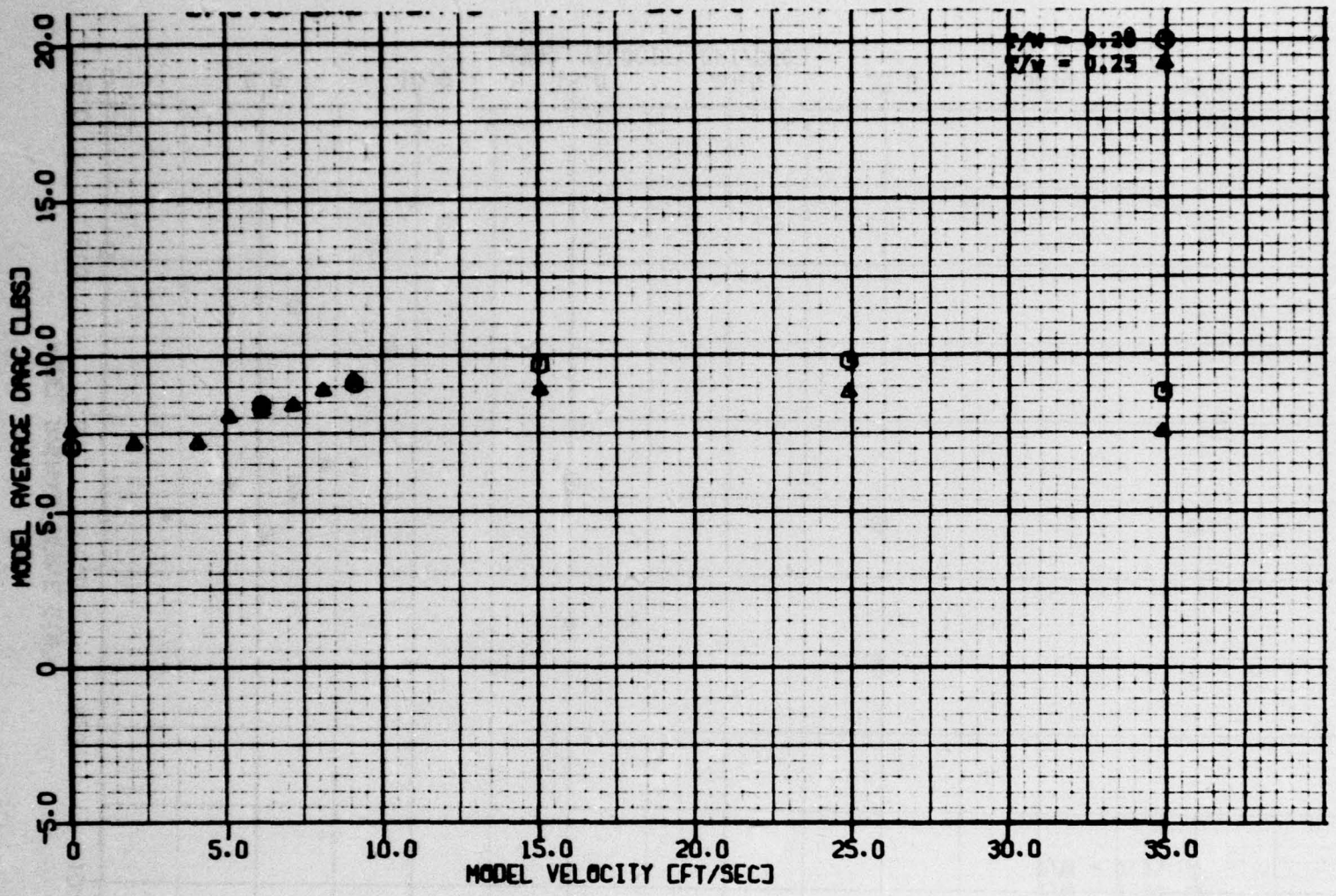

Figure 15b - Model Average Drag Versus Model Velocity

TABLE 1 - PAR-WIG MODEL INFORMATION

	Full-Scale	1/30-Scale
WING		
Airfoil Section	Flat-Bottom NACA 0015	
Chord, c	120 ft (36.58 m)	48 in. (1.22 m)
Span, b	120 ft (36.58 m)	48 in. (1.22 m)
Taper Ratio	1	1
Thickness Ratio	0.15	0.15
RIGID FLAP		
Span		48 in. (1.22 m)
Hinge Line		0.79 c
Angle		40 deg
FLEXIBLE FLAP		
Span		48 in. (1.22 m)
Hinge Line		0.79 c
Fixed Portion Angle		20 deg
Flexible Portion Angle		20 deg
Air Pressure Motor		
Manufacturer		ROTRON INC.
Model Number		367JS
Diameter		2.12 in. (5.38 cm)
Number Used		1
Maximum Output		59 ft^3/min (1.67 m^3/min)
Pressure Range		0-16 lb/ft^2 (0-78 kg/m^2)
PROPULSOR FAN		
Manufacturer		TECH DEV., INC.
Model Number		TD-492
Diameter, D_F		8 in. (20 cm)
Maximum Thrust		37 lb (16.78 kg)
Angle, θ_F		20 deg
Number Used		4

TABLE 1 - (Continued)

	1/30-Scale
NACELLE	
Maximum Diameter	10 in. (25 cm)
Length	4.5 in. (11 cm)
Number Used	4
FUSELAGE	
Length	49 in. (1.24 m)
Width	2 in. (5.08 cm)
Height	2 in. (5.08 cm)
Angle, above mean waterline	2 deg
Number Used	2
BASIC RIGID ENDPLATE	
Maximum Length, ℓ_{ep}	58 in. (1.47 m)
Bottom Length, ℓ	43 in. (1.09 m)
Width, a	1.27 in. (3.23 cm)
Depth Below Wing Bottom	7.12 in. (18 cm)
Deadrise Angle	60 deg
Forebody Planing Surface Length	16.2 in. (41 cm)
Forebody Planing Surface Angle, above mean waterline	21.8 deg
BUMPERS/SPRINGS ENDPLATE	
(BASIC RIGID ENDPLATE PLUS ENERGY ABSORBING FOREBODY)	
Number Springs Used	2
Stiffness, per spring	26, 54, 78, 102 lb/in. (4.6, 9.6, 13.9, 18.2 kg/cm)
SOFT (FLEXIBLE) ENDPLATE	
Maximum Length, ℓ_{ep}	48 in. (1.22 m)
Bottom Length, ℓ	46 in. (1.17 m)
Width, a	2.25 in. (5.71 cm)
Depth Below Wing Bottom	6.89 in. (17.50 cm)
Deadrise Angle	5.5 deg
Forebody Planing Surface Length	5 in. (12.7 cm)
Forebody Planing Surface Angle, above mean waterline	85 deg

TABLE 1 - (Continued)

		1/30-Scale
Flexible Finger Material	0.009 in. (0.23 mm)	nylon, neoprene impregnated
Flexible Finger Number		61
Flexible Finger Pressure Range		0-1 lb/in.^{2} (703.1 kg/m^2)
METAL ENDPLATE		
Maximum Length, ℓ_{ep}		53 in. (1.35 m)
Bottom Length, ℓ		48 in. (1.22 m)
Width, a		0.25 in. (6.3 mm)
Depth Below Wing Bottom		7.75 in. (20 cm)
Deadrise Angle		0 deg
Forebody Planing Surface Length		8.7 in. (22 cm)
Forebody Planing Surface Angle, above mean waterline		30 deg

TABLE 2 - SINGLE SAMPLE ACCURACY

Item	Accuracy
Drag	$\pm$ 0.50 lb ($\pm$ 0.23 kg)
Heave	$\pm$ 0.01 in. ($\pm$ 0.25 mm)
Pressure (Flexible Flap)	$\pm$ 0.50 lb/ft^2 ($\pm$ 2.44 kg/m^2)
Pressure (Soft Endplate)	$\pm$ 0.10 lb/in.^{2} ($\pm$ 70.31 kg/m^2)
RMS Acceleration	$\pm$ 0.01 gravitational units (G)
RMS Heave	$\pm$ 0.01 in. ($\pm$ 0.25 mm)
Velocity	$\pm$ 0.02 ft/sec ($\pm$ 0.02 km/hr)

TABLE 3 - EFFECT OF SEA STATE ON PERFORMANCE OF MODEL WITHOUT LOAD ALLEVIATION

Sea State	Model Weight lb (kg)	$Thrust_{Zero}$ lb (kg)	T/W_{Zero}	$Velocity_{Cruise}$ ft/sec (km/hr)	$Heave_{Cruise}$ in. (cm)
0	87.5 (39.7)	16.98 (7.70)	0.194	44.069 (48.356)	7.75 (19.69)
5	88.5 (40.1)	19.04 (8.64)	0.215	39.929 (43.813)	8.50 (21.59)

Sea State	$Thrust_{Cruise}$ lb (kg)	$V_{j,Cruise}$ ft/sec (km/hr)	P_{Cruise} ft-lb/sec (W)	L/D_{Cruise}	η_T
0	3.192 (1.448)	60.07 (65.91)	166.35 (225.54)	27.41	23.18
5	6.48 (2.94)	68.45 (75.11)	351.14 (476.08)	13.66	10.06